EUROPEAN ORGANIZATION FOR NUCLEAR RESEARCH

CERN-INTC-2006-002
INTC-P-127 Add. 2
17^{th} of January, 2006

Proposal to the Isolde and Neutron Time-of-Flight Committee

Studies of electric dipole moments in the octupole collective regions of heavy Radiums and Bariums

Addendum

Aarhus[1] – CERN[2] – Liverpool[3] – Lund[4] – Madrid[5] – Oslo[6] – Prague[7] – Sydney[8] – Świerk[9] – Uppsala[10]– Valencia[11] – Warsaw[12] – Collaboration

H. Mach[10], P. Alexa[7], M.J.G. Borge[5], H. Bradley[8,10], P.A. Butler[3], J. Cederkäll[2,4], J.L. Egido[5], B. Fogelberg[10], L.M. Fraile[2,4], H. Fynbo[1], P. Hoff[6], R. Kaczarowski[9], U. Köster[2], A. Korgul[12], W. Kurcewicz[12], J. Kvasil[7], A. Płochocki[12], J. Nyberg[10], L. Robledo[5], B. Rubio[11], E. Ruchowska[9], O. Tengblad[5], and J. Żylicz[12]

Spokesman: H. Mach
Contactperson: L. Fraile

Abstract

There is a strong interest in the properties of the exceptionally low first excited state in ^{229}Th. It is proposed to search for the alpha decay branch from the 3.5 eV state in ^{229}Th into the states in ^{225}Ra and to measure its half-life by alpha decay spectroscopy. The expected half-life is of the order of 10 hrs based on our model interpretation of the observed low energy structure in ^{229}Th from our currently completed set of measurements. So far there have been conflicting reports on the half-life or half-life limits for this state. Browne et al. has observed no events and determined the half-life as either below 6 hrs or longer than 20 days, while Mitsugashira et al. has reported the half-life of 13.9±3.0 hrs based on very weak statistics and no firm identification of the origin of the observed counts.

Our proposed measurement will be done at ISOLDE by using different population of the metastable state in ^{229}Th than done in the previous measurements. In this respect the mass separation technique at ISOLDE represents a unique production technique, and could offer a significant advantage. We ask for 4 new shifts of radioactive beams (A=229, but mainly ^{229}Ra), which will be combined with 2 shifts left for the IS386 collaboration from the previous year.

1. Motivation

The motivation for the detailed investigation of the low-energy structure of ^{229}Th has been included in our original beam proposal for the IS386 project and moreover it is also presented in detail in Appendix I, which is a copy of our publication on ^{229}Th recently submitted for publication. (On January 20-th, 2006, this paper has been tentatively accepted for publication in Physical Review C.) Consequently, the following presentation highlights only the key aspects related to motivation.

Precision γ-spectroscopy studies performed by Helmer and Reich [1] on the ^{233}U $\rightarrow$ ^{229}Th alpha decay place the first excited state of the daughter nucleus at unusually low energy of 3.5$\pm$1.0 eV. The spin and parity of this state is presumably $3/2^+$, while that of the ground state is $5/2^+$. These two states are interpreted as the $3/2^+[631]$ and $5/2^+[633]$ Nilsson-model orbitals. The $3/2^+$ state is expected to be an isomer. Its partial γ-decay half-life has been estimated to be in the range of hours, see [2] and Appendix I.

There are at least two reasons for a special interest in the 3.5 eV $3/2^+$ state. First, it offers a unique possibility to study coupling between the nuclear and atomic degrees of freedom [3, 4, 5]. Second, it gives a chance to observe the nuclear-spin mixing that is expected to take place in case of hydrogen-like ions ^{229}Th^{89+} circulating in a storage ring [2, 5], e.g.: ESR at GSI.

The first effect can manifest itself via the so-called electronic bridge [3]. It means a competition to the γ-decay from a two-step process: a part of the excitation energy is transferred to one of the valence electrons to shift it to another orbit. The rest of the energy is carried away by a "red-shifted" γ-ray photon. The enhancement of the isomeric transition depends upon its energy. As predicted by the theory [5], it can be as high as three orders of magnitude [5]. To verify this theory one needs (i) the isomer energy with uncertainty below $\pm$0.1 eV, (ii) the half-life of the isomer in a neutral atom, and (iii) the partial half-life for the isomeric M1 γ transition. For predictions of the mixing of the $5/2^+$ ground state and the $3/2^+$ isomeric state in a hydrogen-like ion of ^{229}Th one needs additionally the magnetic-moment value for the isomer.

We have originally proposed to reinvestigate the β and γ spectroscopy of the ^{229}Ac to ^{229}Th decay, with a special effort to measure subnanosecond lifetimes of the excited states in ^{229}Th. Theoretical analysis of data obtained for the rotational bands build on the $K^\pi=5/2^+$ ground state and on the $\approx$3.5 eV $3/2^+$ isomer did allow to derive the partial γ-decay half-life of this isomer, of about 10 hrs, as presented in Appendix I. There has been no unambiguous measurement of this lifetime. In fact, there have been two reported measurements which results exclude one another. Browne et al.[6] has observed no events and determined the half-life as either below 6 hrs or longer than 20 days, while Mitsugashira et al.[7] has reported the half-life of 13.9$\pm$3.0 hrs based on very weak statistics and no firm identification of the origin of the observed counts.

2. Proposed alpha-spectroscopy of the decay of ^{229}Th^m

The A=229 activity will be produced in a proton-induced spallation of ^{238}U and mass separated. The A=229 isobars form a chain of the β-decays:

$$^{229}\mathrm{Fr}(50\ \mathrm{s}) \rightarrow {}^{229}\mathrm{Ra}(4.0\ \mathrm{min}) \rightarrow {}^{229}\mathrm{Ac}(1.04\ \mathrm{hr}) \rightarrow {}^{229}\mathrm{Th}.$$

The dominant production activity will be ^{229}Ra (about a 2–6 $\times$ 10^6 /s) and ^{229}Fr (about

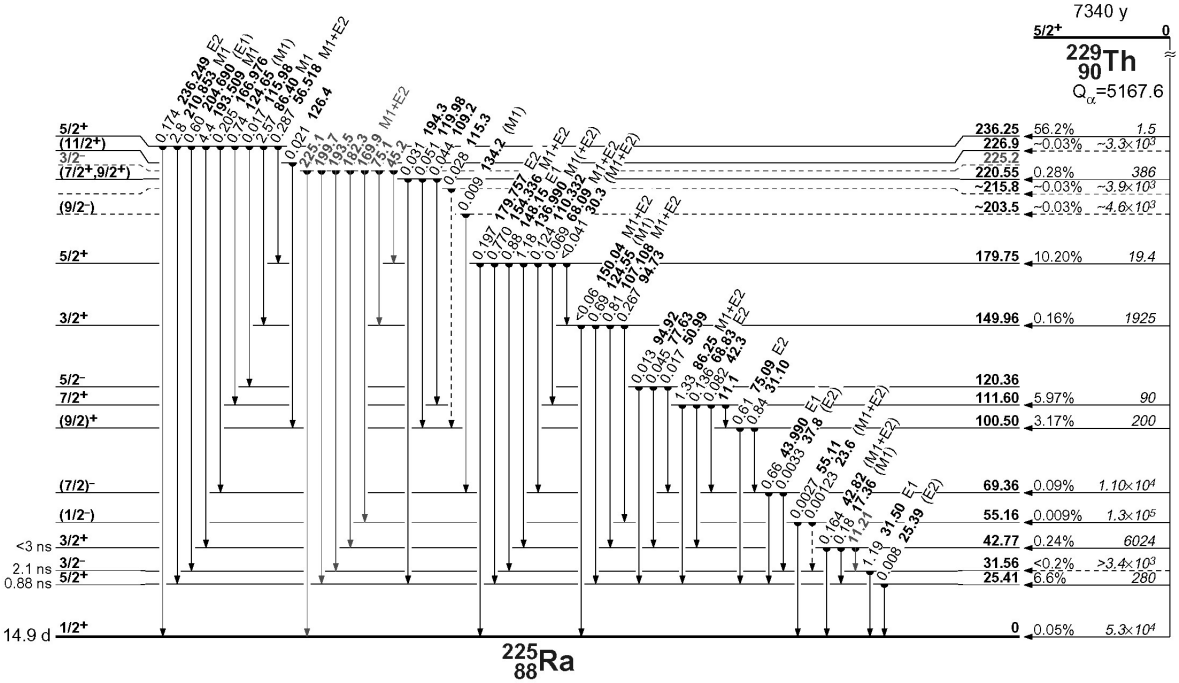

Figure 1: A partial alpha-decay scheme of ^{229}Th to ^{225}Ra.

1–2 $\times$ 10^5/s). We expect that the beta decay of ^{229}Ac will populate the metastable state at 3.5 eV with about 50% probability, out of which only a tiny fraction will proceed via an alpha decay. This branching is estimated next.

The 5/2+[633] ground state of ^{229}Th decays by an unhindered alpha transition to the 0.236 MeV 5/2+[633] state in ^{225}Ra with $T_{1/2}$ of 7880 years = 2.49 $\times$ 10^{11} s, with the branching of 56% and the energy of Q_α=5.1679 MeV, see Fig. 1.

On the other hand the decay of the 3/2+ [631] 3.5 keV isomer of ^{229}Th should decay predominantly by an unhindered transition to the 0.150 MeV 3/2+[631] state in ^{225}Ra with similar parameters, which due to the energy factor should yield 1.23 $\times$ 10^{11} s as partial half-life and 6.9 $\times$ 10^{10} s as total half-life for the alpha decay to ^{225}Ra. Assuming that the half-live of the level is 10 hrs (3.6 $\times$ 10^4 s), then the alpha branching is only 5.2 $\times$ 10^{-7}.

Although there will be some short test irradiations, yet we expect that two strong radioactive sources will be irradiated (one at LA1 and one at LA2 beam lines) each over 22-24 hours, with the cooling time of about 14 hours to minimize the beta decay of ^{229}Ac. With the beam strength of 1 $\times$ 10^6 atoms/s, we will produce about 8 $\times$ 10^{10} atoms of ^{229}Th with about 50% in the metastable state. After the cooling time of 14 hrs, we will have as the most significant problem the beta activity from the decay of ^{229}Ac at about 2 $\times$ 10^5 dps, which will decay much faster than the alpha activity and will have much lower energy, which can be cut by raising the threshold in the detector system.

Overall about 20 000 events of interest (alphas from the metastable state) will be produced, of which about 90% will decay by the time the cooling period ends. This would still leave about 1000-2000 alphas to be observed in a direct decay. Our alpha detector efficiency will be about 30–35%.

As alpha detectors we will have standard Si-detectors, but also scintillators (thin plastic or BaF_2 discs), with the measurements conducted in a small vacuum chamber. The scintillators can be used at very high counting rates for beta-rays, making the measure-

ment sensitive to shorter lifetimes of the isomer. The main measurement will be the multispectrum scalling of alpha events as a function of decay time. The resolution of the alpha spectrum will depend on the alpha detector used. The measuring station will also include a small Ge detector, working in coincidence with alpha detector.

In principle, besides the contribution from beta-rays recorded at low energies, the energy spectra should include only the alpha lines present from the long-lived ground state decay of ^{229}Th and the shorter-lived component from the isomeric state. The decay of ^{225}Ra has a half-life of 14.9 days, thus the short-lived component of the metastable state in ^{229}Th should be easily extracted from the long-lived components using the time evolution of the energy spectra.

4. Summary of beam requests

In total, we request 4 new shifts with radioactive beams, this will be combined with 2 shifts left to the project from previous year. We request the use of ThC target. We will need 1 shift of stable beam to align the beam lines.

Nucleus	# of shifts	Separator	Target	Ion source	Min.Intensity
Stable beam	1	GPS/HRS	ThC	WSI	
^{229}Ra	6	GPS/HRS	ThC	WSI	1x10^6
total new shifts	4				

References

[1] R.G. Helmer and C.W. Reich, Phys. Rev. **C49** (1994) 1845, and references therein.
[2] S. Wycech and J. Zylicz, Acta Phys. Pol. **B24** (1993) 637.
[3] E.V. Tkalya, Pisma Zh. Eksp. Teor. Fiz. **55** (1992) 216, [JETP Lett. **55** (1992) 211].
[4] F.F. Karpeshin *et al.*, Phys.Lett. **B282** (1992) 267.
[5] F.F. Karpeshin *et al.*, Phys. Rev. **C57** (1998) 3085.
[6] E. Browne *et al.*, Phys. Rev. C **64**, 014311 (2001).
[7] T. Mitsugashira *et al.*, J. Radioanal. Nucl. Chem. **255**, 63 (2003).

Nuclear Structure of ^{229}Th

E. Ruchowska,[1,*] W.A. Płóciennik,[1,†] J. Żylicz,[2] H. Mach,[3] J. Kvasil,[4] A. Algora,[5] N. Amzal,[6] T. Bäck,[7] M.G. Borge,[8] R. Boutami,[8] P.A. Butler,[6] J. Cederkäll,[9] B. Cederwall,[7] B. Fogelberg,[3] L.M. Fraile,[9,‡] H.O.U. Fynbo,[9] E. Hagebø,[10] P. Hoff,[10] H. Gausemel,[10] A. Jungclaus,[8] R. Kaczarowski,[1] A. Kerek,[7] W. Kurcewicz,[2] K. Lagergren,[7] E. Nacher,[5] B. Rubio,[5] A. Syntfeld,[1] O. Tengblad,[8] A.A. Wasilewski,[1] and L. Weissman[9]

[1] *The Andrzej Sołtan Institute for Nuclear Studies, PL 05-400 Świerk, Poland*
[2] *Institute of Experimental Physics, University of Warsaw, PL 00-681 Warsaw, Poland*
[3] *Department of Radiation Sciences, University of Uppsala, SE-751 21 Uppsala, Sweden*
[4] *Department of Nuclear Physics, Charles University, 18000 Prague 8, Czech Republic*
[5] *Instituto de Fízica Corpuscular, CSIC-University Valencia, E-46100 Burjassot, Spain*
[6] *Oliver Lodge Laboratory, University of Liverpool, Liverpool L69 3BX, United Kingdom*
[7] *Physics Department, Royal Institute of Technology, SE-106 91 Stockholm, Sweden*
[8] *Instituto de Estructura de la Materia, CSIC, E-28006 Madrid, Spain*
[9] *ISOLDE, CERN, CH-1211 Geneva 23, Switzerland*
[10] *Department of Chemistry, University of Oslo, P.O. Box 1033 Blindern, N-0315 Oslo, Norway*

(Dated: December 22, 2005)

Lifetimes of excited states in ^{229}Th, populated in the β decay of ^{229}Ac, have been measured using the Advanced Time-Delayed $\beta\gamma\gamma$(t) method. Half-lives of 14 states have been determined including 11 of them for the first time. Twenty-seven new γ-lines have been introduced into the β-decay scheme of ^{229}Ac based on results of $\gamma\gamma$ coincidence measurements. Reduced transition probabilities have been determined for more than 70 γ-transitions in ^{229}Th. Average $|D_0|$ values of 0.029(1), 0.077(3) and 0.024(5) efm have been deduced for the lowest $K^{\pi}=1/2^{\pm}$, $3/2^{\pm}$ and $5/2^{\pm}$ parity partner bands, respectively. Excited states in ^{229}Th and experimental transition rates have been interpreted within the quasiparticle-plus-phonon model. The half-life of the 3.5 eV, $3/2^{+}$ isomeric state is predicted to be about 10 h. Potential energy surfaces on the (β_2,β_3) plane for the lowest single quasiparticle configurations in ^{229}Th have been calculated using Strutinsky method.

PACS numbers: 21.10.Tg; 21.10.Re; 21.10.Ky; 27.90.+b

I. INTRODUCTION

Spectroscopic studies of the ^{229}Th nucleus are very important at least for two reasons. Firstly, ^{229}Th lies at the perimeter of the octupole deformation region in Actinides and the coexistence of reflection-symmetric and reflection-asymmetric shapes is expected in this nucleus [1]. Secondly, the first excited state in ^{229}Th at the energy of only 3.5(10) eV [2] is the lowest excited state known in all nuclei and the only one with excitation energy within the atomic energy scale (recent evaluation [3] gives the energy of 5.5(10) eV for this state). Consequently the lowest excited state in ^{229}Th presents a unique opportunity to investigate interactions between nuclear and atomic degrees of freedom and was the main subject of several works in the last few years (e.g. [4–7] and references quoted therein). While a direct observation of this state has not yet been possible, an estimate of its properties can be obtained by extrapolation from properties of the higher-lying levels in ^{229}Th.

Excited states in ^{229}Th have been previously studied in the α-decay of ^{233}U [8, 9], β-decay of ^{229}Ac [10], electron-capture decay of ^{229}Pa [11] as well as in the transfer reactions [12, 13] and Coulomb excitations [14]. Recently new studies on the β-decay of ^{229}Ac [15] and on the α-decay of ^{233}U [16] have been reported. Multipolarities of many γ-transitions in ^{229}Th have been established in Ref. [15] by internal-conversion electron measurements. Lifetimes of the 42.3 and 97.1 keV levels have been measured in Ref. [17] and of the 146.4 and 164.5 keV levels in Ref. [15]. Despite a large body of experimental data on ^{229}Th only the structure of levels below 300 keV is clearly understood. In order to obtain a better understanding of the low energy structure of ^{229}Th we have measured lifetimes of the excited states in this nucleus using the Advanced Time-Delayed $\beta\gamma\gamma(t)$ method [18–20]. The experimental methods are briefly described in Section II, while the new level scheme for ^{229}Th and the lifetime results are presented in Section III of this paper. In Section IV experimental results are discussed in terms of the quasiparticle-plus-phonon model. Additionally results of potential energy calculations on the (β_2,β_3) plane are also presented.

II. EXPERIMENTAL DETAILS

Measurements were carried out at the High Resolution Mass Separator (HRS) at the ISOLDE facility at CERN. Excited states in ^{229}Th were populated in the β-decay

*ewa@ipj.gov.pl
†deceased
‡On leave from Universidad Complutense, E-28040 Madrid, Spain

of ^{229}Ac, which was obtained via a chain of β-decays starting from the ^{229}Fr isotope

$$^{229}Fr \overset{50s}{\rightarrow} {}^{229}Ra \overset{4.0m}{\rightarrow} {}^{229}Ac \overset{62.7m}{\rightarrow} {}^{229}Th.$$

The ^{229}Fr nuclei were produced in the spallation reaction of ^{238}U induced by the 1.4 GeV protons from the PS booster. The ^{229}Fr activity mass separated from other spallation reaction products, was implanted onto an aluminium foil. After about 40 min of irradiation and 30 min of cooling time, foil with almost pure activity of ^{229}Ac was placed in the center of our experimental setup.

Level lifetimes in the sub-nanosecond range have been measured with the Advanced Time-Delayed $\beta\gamma\gamma$(t) method [18–20]. Fast timing information was derived from time-delayed coincidences between fast-response β- and BaF_2 γ-detectors, while additional coincidences with a Ge γ-detector were used to select the desired γ-cascade. A 3 mm thick plastic scintillator NE111A was used as β-detector to ensure for it a constant time response independent of energy of incident β-particles. The setup consisted of two BaF_2 detectors in shape of truncated cones with height of 2.5 cm each and two HPGe detectors with efficiencies of about 40% and 70%, respectively. This resulted in one combination of β-Ge-Ge coincidences, which served to construct the level scheme, and four combinations of β-Ge-BaF_2 coincidences which provided lifetime information. Triple and higher-fold coincident events were collected and then pre-sorted off-line into data sets with triple coincidences mentioned above. Two independent series of measurements were performed, in which about 3.7×10^6 and 8.4×10^6 triple coincidence events were collected, respectively.

III. EXPERIMENTAL RESULTS

A. Level scheme

The results for ^{229}Th are presented in Figs. 1 − 4 and in Table I. The level scheme was constructed based on the β-Ge-Ge data. Examples of coincident γ-ray spectra collected with the Ge detectors are shown in the upper panels of Figs. 1 − 3, while the new level scheme for ^{229}Th is presented in Figs. 4a−c. Level and gamma-ray energies determined in the present work are given in columns 1 and 4 of Table I, respectively, and also in the level scheme. For several γ-lines precise γ-ray energies were adopted from Ref. [2]. Some of these energies were used for internal energy calibration which served to determine the energies of other lines in ^{229}Th. Where available, γ-ray intensities as well as E2/M1 mixing ratios were taken from Ref. [15] (the intensity relations in our data have been distorted by the low-energy cut-off in the gating β signals).

In general our level scheme for ^{229}Th agrees well with the one obtained by Gulda *et al.* [15]. The exception is the 526.75 keV level, for which no evidence was found in our data. Twenty-seven new γ-lines have been introduced into the decay scheme of ^{229}Ac connecting levels already established in previous works. Six of them have already been observed in the α-decay of ^{233}U [16]. New lines are marked by stars in Figs. 4a−c and in Table I. Information on new transitions not listed in Table I is given in Table II. Highly converted transitions, which have not been directly observed in our spectra but whose existence has been established from our coincidence data, are drawn with dashed lines in the level scheme and are given in parentheses in Table I. For completeness, transitions seen by Gulda *et al.* [15] but not observed in our data because of lower efficiency of our setup in the very low and high energy ranges or due to restrictive coincidence requirements, are shown in the level scheme by dotted lines.

B. Level lifetimes

Level lifetimes were determined from the analysis of the triple coincidence β-Ge-BaF_2 data. The key to the analysis is a clean separation of the full energy peaks in the gating spectra. Examples of γ-ray BaF_2 spectra coincident to the gating transitions selected in the Ge detector are shown in the lower panels of Figs. 1 − 3.

1. *Slope fitting*

Lifetimes longer than about 40 ps, which manifest themselves by strong asymmetry (or slope) on the delayed side of the time spectra, have been measured using the de-convolution method [18]. This method is frequently called *slope fitting* from its simplest form of analysis. Examples of such time-delayed spectra are those obtained for the 146.4, 148.2 and 424.0 keV levels in ^{229}Th as shown in Fig. 5. The fitted function includes four free parameters, namely position and Full-Width-at-Half-Maximum of Gaussian, which approximates prompt time response of the timing detectors, the half-life value and one parameter, which provides an overall re-normalization between the experimental and fitted time spectra. More details on the fitting procedures are given in Ref. [18].

As an example of the analysis consider the half-life of the 146.4 keV level. As seen in Fig. 1 the 146.4 keV level is strongly fed from above by the 422.9 keV transition, which can be very clearly identified also in the corresponding BaF_2 coincident spectrum despite of poor energy resolution of BaF_2 detectors. By reversing the gates and selecting the 422.9 keV transition in the Ge detector, see Fig. 3, one can unambiguously select in the BaF_2 spectrum the 117.2 and 146.3 keV transitions de-exciting the 146.4 keV level. Then by selecting the energy gate in this spectrum covering the full energy peaks due to the 117.2 and 146.3 keV transitions, one obtains the time-delayed β-BaF_2(t) spectrum shown in the top panel of

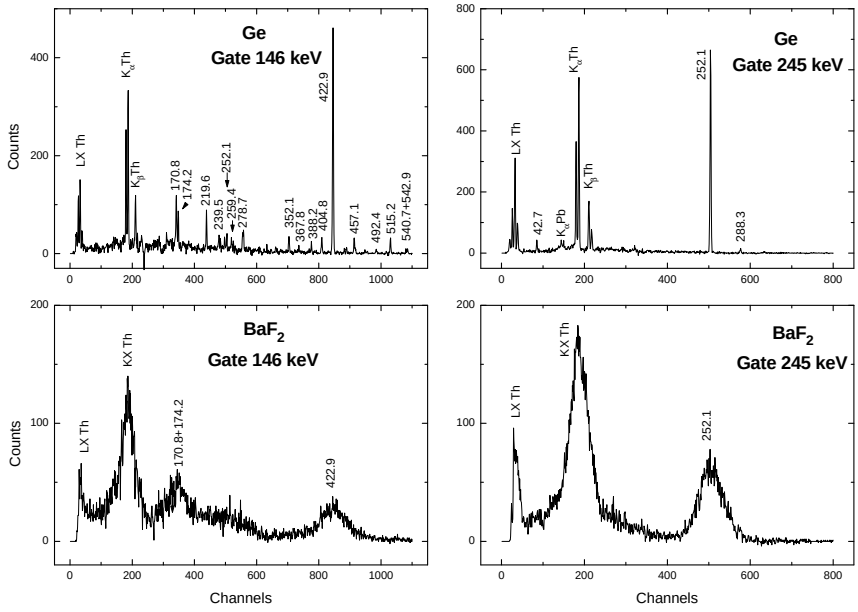

FIG. 1: Top panels show coincident γ-ray Ge spectra sorted from the β-Ge-Ge data using gates set on the 146.3 (left) and 245.3 keV transitions (right). Panels at the bottom show the corresponding coincident γ-ray spectra sorted onto the BaF_2 detector using the β-Ge-BaF_2 data.

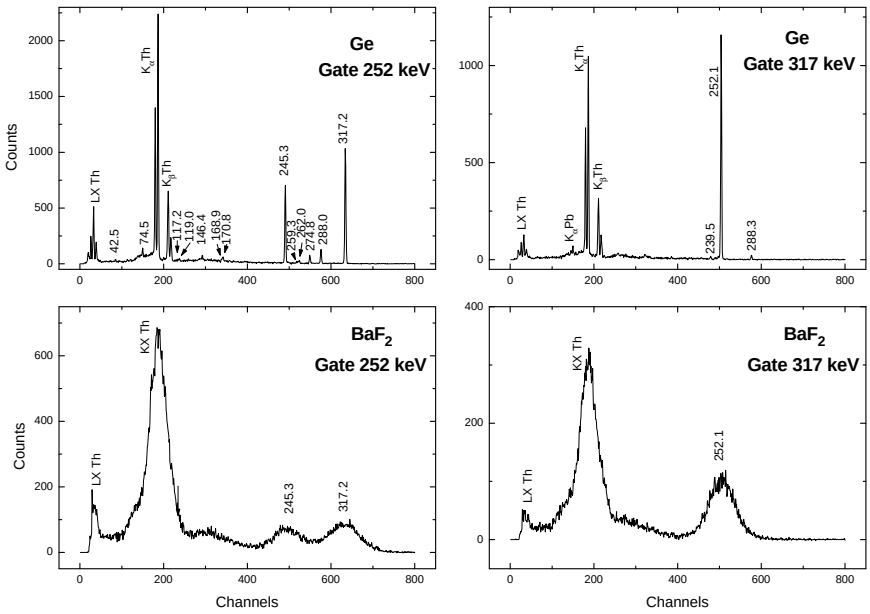

FIG. 2: Similar to Fig. 1 but gated on the 252.1 and 317.2 keV transitions.

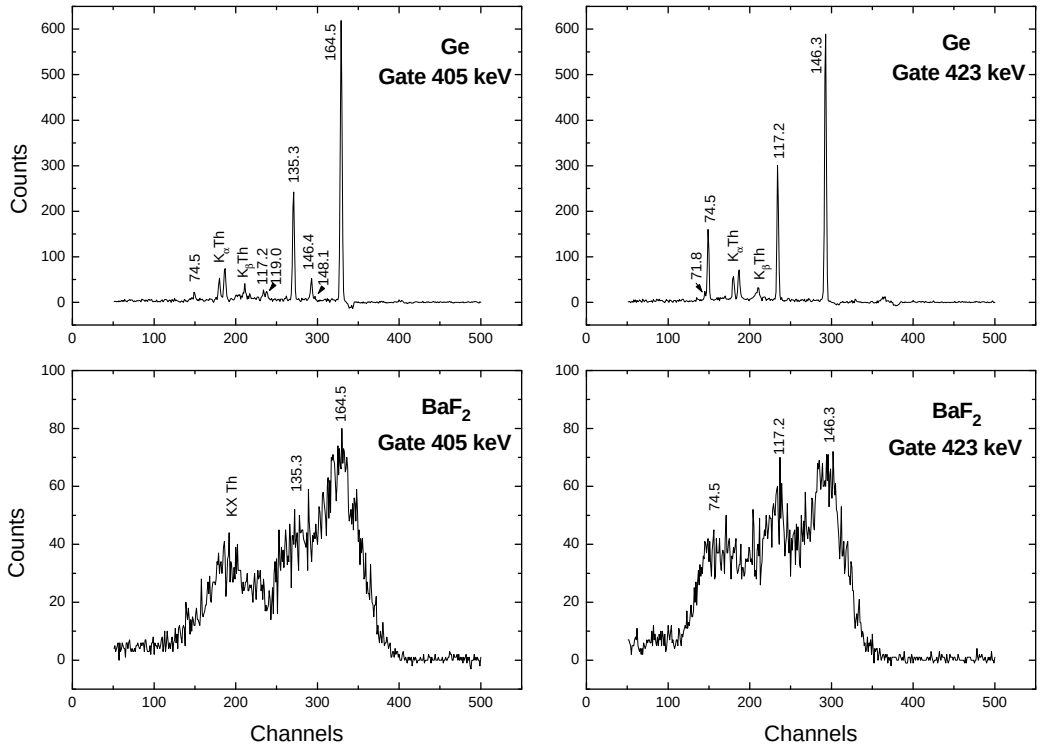

FIG. 3: Similar to Fig. 1 but gated on the 404.8 and 422.9 keV transitions.

Fig. 5. We note here, that all spectra shown in Figs. 1 − 3 and 5 were also gated on the β detector using one common energy gate. In the γ cascades selected for analysis care was taken to ensure that γ-rays feeding the state of interest from above de-excite levels with lifetimes much shorter than the measured lifetime and do not interfere in the de-convolution process.

The time spectrum shown in Fig. 5 represents in fact a sum of similar time distributions gated in Ge detector on the 219.6, 422.9 and 515.2 keV transitions feeding directly the 146.4 keV level from above. The half-lives determined individually from their time distributions are the same within the uncertainties, nevertheless the contributions related to the 219.6 and 515.2 keV transitions have much weaker statistics than that for the 422.9 keV line, and thus influence in a minor way the final value for the half-life of the 146.4 keV level.

The half-lives for the levels at 146.4, 148.2, 164.5, 303.0, 424.0 and 425.3 keV have been determined by the de-convolution method, as 329(8) ps, 689(34) ps, 61(7) ps, 110(17) ps, 190(8) and 290(48) ps, respectively. These results were obtained in the second run, characterized by higher statistics and slightly better energy resolution in Ge detectors. For a comparison we list the half-lives of $T_{1/2}$ = 332(18) ps, 677(62) ps, 62(11) ps and 175(18) ps obtained for the 146.4, 148.2, 164.5 and 424.0 keV levels, respectively, in the first run. Moreover, our half-life results measured for the 146.4 and 164.5 keV levels from triple coincidence β-BaF_2-Ge events nicely confirm the values of 336(10) and 53(4) ps obtained for these levels by Gulda *et al.* [15] in a less restrictive way from double β-BaF_2(t) coincidences.

2. Centroid-shift analysis

Lifetimes shorter than 40 ps were measured using the centroid shift method [18], in which the mean lifetime τ=$T_{1/2}$/ln2 is determined as shift of the centroid of the time-delayed spectrum from the prompt curve at a given γ-ray energy. Centroid shift measurements in this work are based on the concept of a two γ-ray cascade [18]. The method is illustrated using an example of the 317.2 keV level, for which the shortest and the most precise result has been obtained.

Consider the cascade involving the 252.1 and 317.2 keV transitions de-exciting the 569.3 keV level to the ground state via the 317.2 keV intermediate state, lifetime of which is to be determined. As seen in Fig. 2 by gating on the 317.2 keV transition in the Ge detector, one

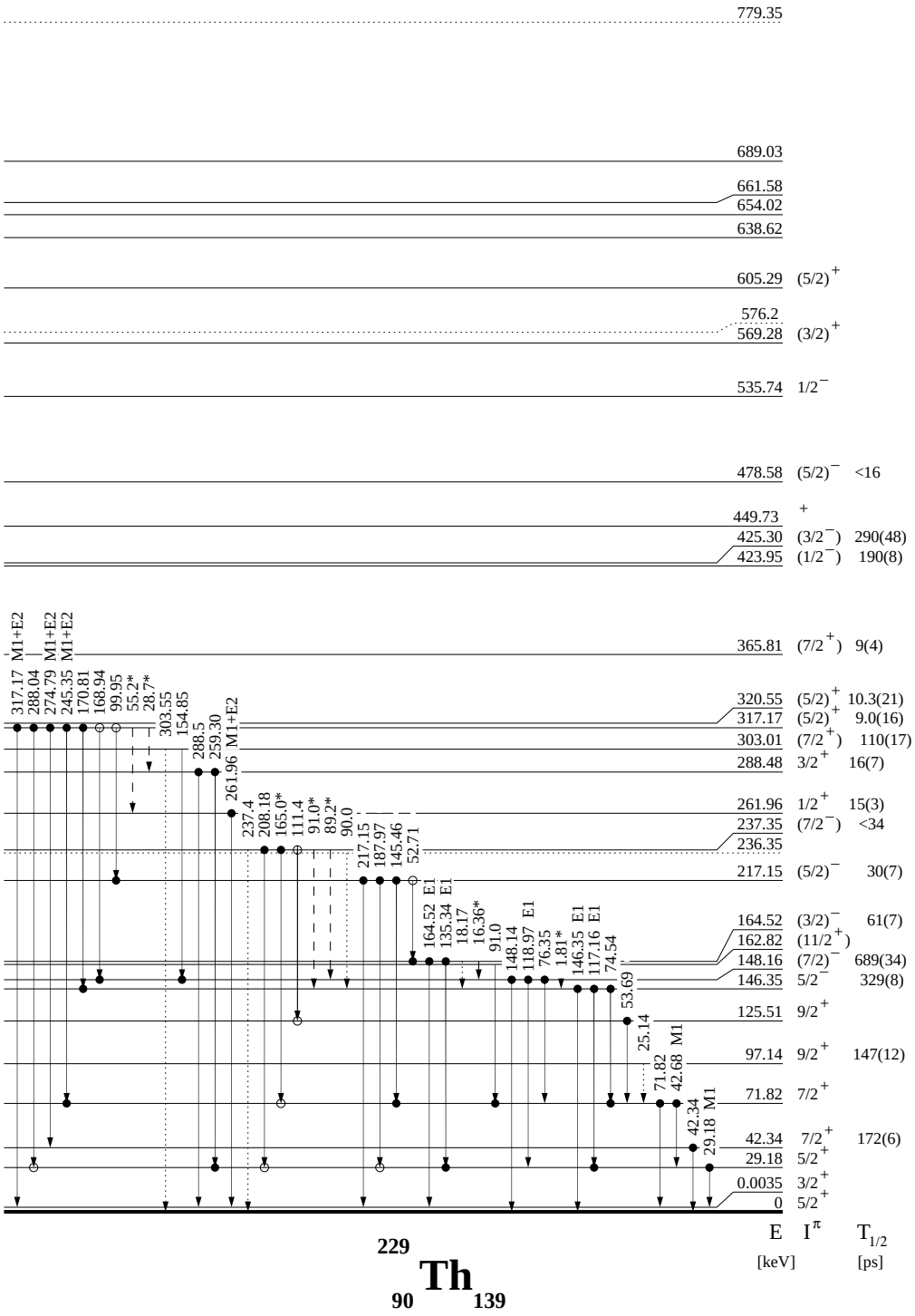

FIG. 4: The level scheme of ^{229}Th from the β decay of ^{229}Ac. Full and empty circles indicate strong and weak $\gamma\gamma$ coincidence relations, respectively. Dotted lines mark transitions seen in Ref. [15] but not observed in our data, while dashed lines show highly converted and unobserved transitions established on the basis of our coincidence relations. Stars indicate new transitions in the β decay of ^{229}Ac observed in this work. Lifetimes for the 42.3 and 97.1 keV levels are taken from Ref. [17].

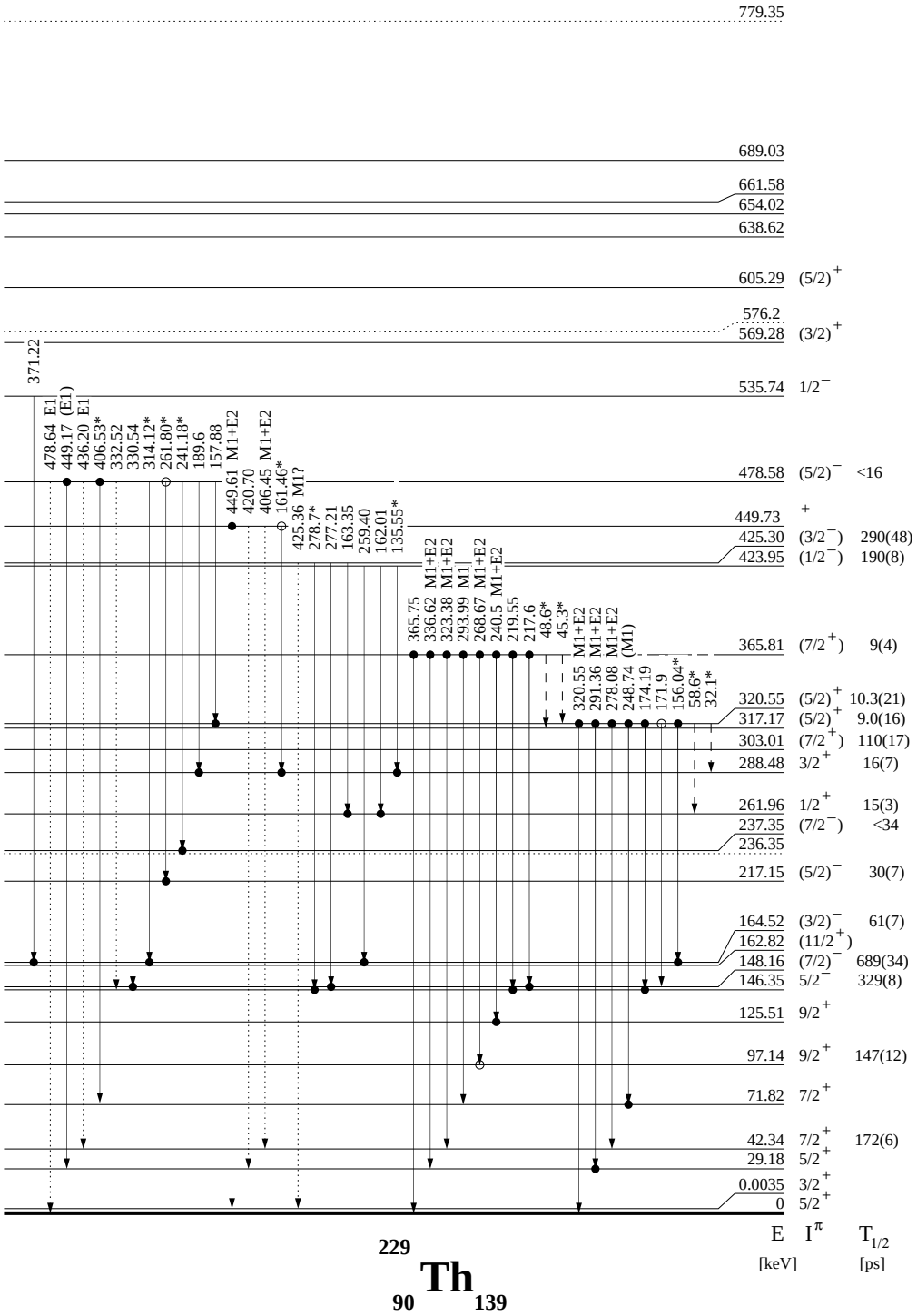

Fig. 4: *(Continued).*

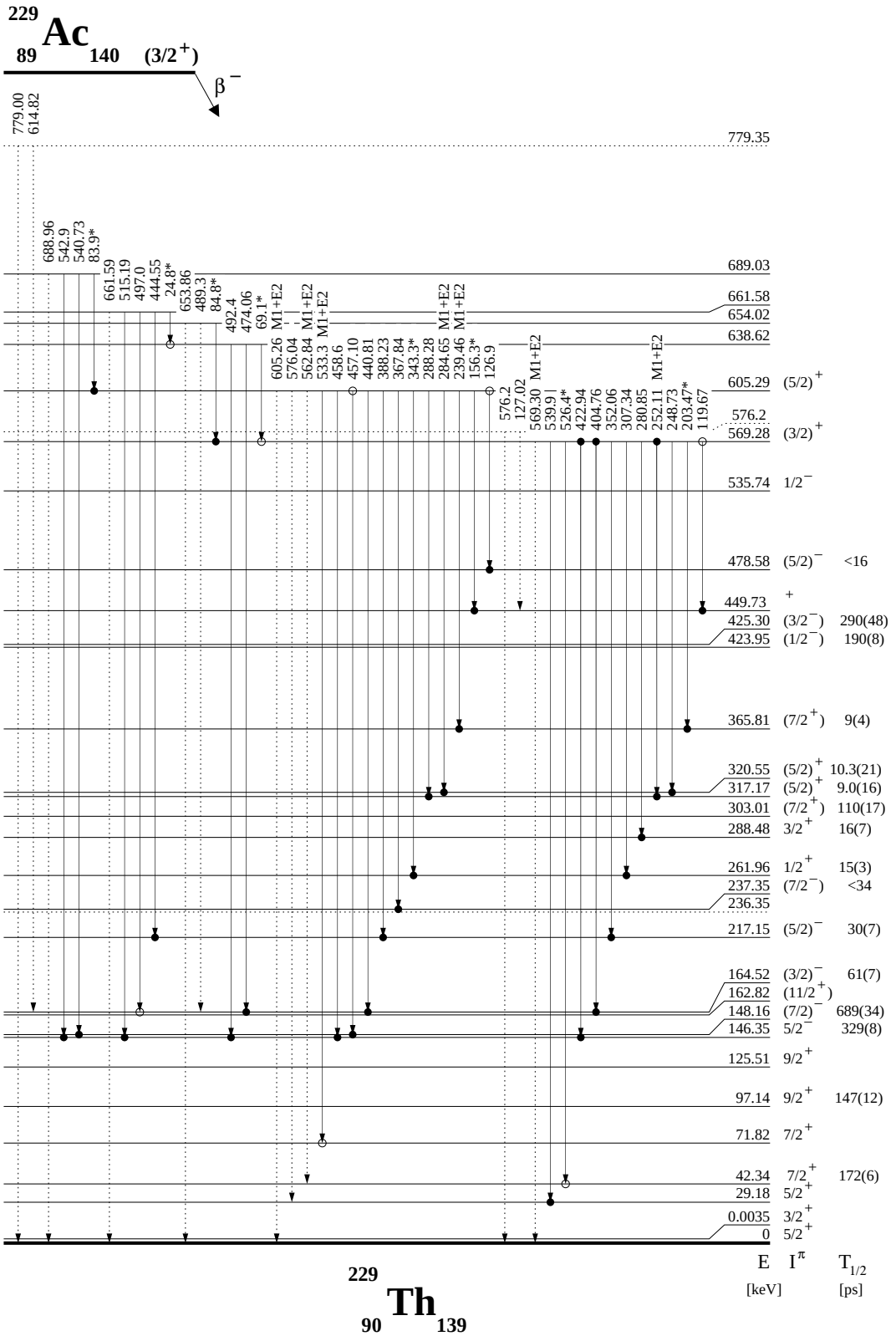

Fig. 4: *(Continued).*

is able to select the very strong 252.1 keV transition in the BaF_2 spectrum and determine the centroid position of the resultant time-delayed β-BaF_2(t) spectrum. This position represents our reference point, which is shown on the *reference curve* in Fig. 6 at the energy of 252 keV. (Similarly, one can use the time spectrum generated by the 245.3 keV (Ge) and the 252.1 keV (BaF_2) gates, see Fig. 1, to confirm the reference point at 252 keV.) We do not know the lifetime of the 569.3 keV level or levels above it, which feed this state. For the purpose of present analysis these lifetimes do not have to be determined since they cancel out in the analysis.

By reversing the gates and selecting the 252.1 keV transition in Ge detector, see Fig. 2, one can gate on the full energy peaks due to the 245.3 and 317.2 keV γ-rays de-exciting the 317.2 keV level. By selecting these transitions in the BaF_2 energy spectrum one obtains the time-delayed β-BaF_2(t) distributions, centroids of which are shifted from the reference point by exactly the mean-life of the 317.2 keV level. As shown in the middle panel of Fig. 6 these points, labelled 252-245 and 252-317, are shifted above the reference curve.

As seen in the figure, a single reference point at one γ-ray energy (say at 252 keV) will not allow for a precise lifetime determination if the time-shifted point is measured at another energy (say 317 keV), unless a reference curve is established over a wider energy range. A second point can be easily established at 423 keV by using the Ge gate at 146.3 keV and selecting the 422.9 keV transition in the BaF_2 spectrum, see Fig. 1. Since this transition de-excites the same 569.3 keV level as the 252.1 keV γ-ray, thus the centroid of the time spectrum selected with the 146.3 keV (Ge) and 422.9 keV (BaF_2) transitions represents exactly the position of the reference curve at 423 keV. We note that the reference curve is relatively flat in the energy range from 252 to 423 keV, which would allow to complete the measurement for the 317.2 keV level using only two reference points. However, by using different combinations of gates set on the full-energy peaks in the Ge and BaF_2 spectra on transitions de-exciting the 569.3 keV level we have extended the reference curve. Moreover, a similar curve was established for transitions de-exciting the 605.3 keV level. Since, within the high level of precision, there was no detectable shift between these curves we have merged them into one reference curve shown in Fig. 6.

We have used three time-delayed points to determine the half-life of the 317.2 keV state. The third point was set on the energy of 288 keV in the BaF_2 spectrum. This gate includes not only the full energy peak of the 288.0 keV γ-ray but also contributions from other weaker lines at this energy and partial contribution from the full energy peaks at 245.3 and 317.2 keV. Since all these transitions de-excite the same level at 317.2 keV and contribution from the Compton tail is minor at these energies, therefore there was no need for any correction procedures.

We finally note, that since all time-delayed spectra were started with detection of β particle, the gating conditions on the β-spectrum were chosen to keep the time response of β detector constant to within $\sim$1 ps over the range of selected β particle energies.

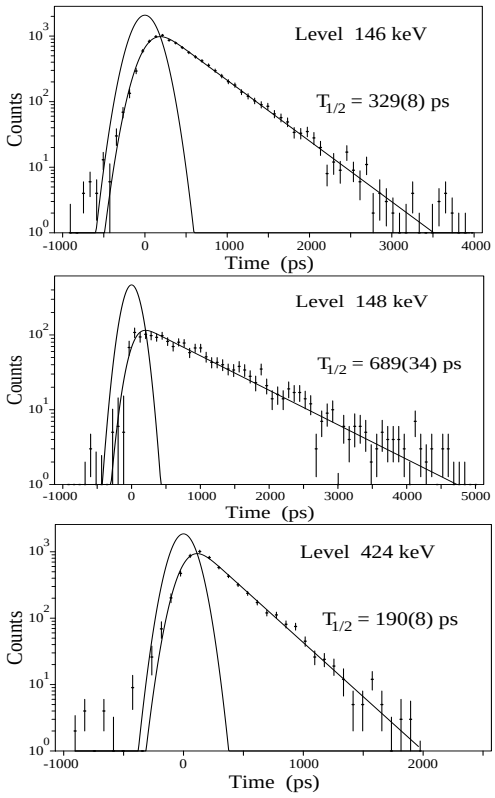

FIG. 5: Time-delayed $\beta\gamma\gamma$(t) spectra showing slopes due to the lifetimes of the 146.4, 148.2 and 424.0 keV levels in ^{229}Th. Each figure shows experimental points, prompt Gaussian spectrum and slope curve, which was fitted in the deconvolution process.

3. Transition rates

Half-life results obtained in the present work are shown in the level scheme and are listed in the third column of Table I. Reduced transition probabilities for about 70 transitions in ^{229}Th are given in column 9 of Table I. Most of them were established in this work. They were determined from level lifetimes and relative γ-ray intensities using total internal conversion coefficients from Ref. [21]. For transitions with energies below 21 keV total internal conversion coefficients were taken from Ref. [22]. For the 1.8 keV transition, assumed to be of M1 type, total internal conversion coefficient of $\alpha_{tot} = 8500$ was

TABLE I: Level lifetimes and experimental and theoretical reduced transition probabilities in ^{229}Th; γ-ray energies are determined in this work unless noted otherwise. New γ-lines are marked by stars.

Initial level [keV]	$I_i K_i^\pi$	$T_{1/2}$ [ps]	E_γ [keV]	I_γ [a]	$I_f K_f^\pi$	$X\lambda$ [a]	α_{TOT} [b]	$B_{exp}(X\lambda)$ [c]	$B_{theor}(X\lambda)$
0.0035	3/2 3/2$^+$		(0.0035)		5/2 5/2$^+$	M1			2.5×10^{-2}
						E2			5.6×10^{3}
29.18	5/2 3/2$^+$		29.1846(30) [d]	1.98(8)	3/2 3/2$^+$	M1			1.1×10^{-2}
						E2			1.9×10^{4}
			(29.18)		5/2 5/2$^+$	M1			0.9×10^{-2}
						E2			4.1×10^{3}
42.34	7/2 5/2$^+$	172(6) [e]	42.34(10)	0.44(9) [f]	5/2 5/2$^+$	M1 [g]	48.0	$1.8(5)\times10^{-2}$	1.52×10^{-2}
						E2 [g]	720	$2.4(15)\times10^{4}$	3.19×10^{4}
71.82	7/2 3/2$^+$		29.36 [g]		7/2 5/2$^+$	M1			0.7×10^{-2}
						E2			3.7×10^{3}
			42.68(4)	0.5	5/2 3/2$^+$	M1			1.4×10^{-2}
						E2			1.1×10^{4}
			71.8159(20) [d]	0.40(2)	3/2 3/2$^+$	E2			0.7×10^{4}
			(71.82)		5/2 5/2$^+$	M1			0.5×10^{-2}
						E2			3.1×10^{3}
97.14	9/2 5/2$^+$	147(12) [e]	25.14(10) [h]	0.65(3)	7/2 3/2$^+$	M1	210	$3.8(4)\times10^{-2}$	8.56×10^{-3}
			54.699(1) [g]	1.94(32) [g]	7/2 5/2$^+$	M1 [g]	21.5	$9.2(19)\times10^{-3}$	1.61×10^{-2}
						E2 [g]	200	$9.3(27)\times10^{3}$	5.13×10^{3}
			67.943(6) [g]	0.17(4) [g]	5/2 3/2$^+$	E2	70	$1.6(4)\times10^{3}$	930
			97.134(1) [g]	2.17(49) [g]	5/2 5/2$^+$	E2	14.0	$3.4(8)\times10^{3}$	2.09×10^{3}
125.51	9/2 3/2$^+$		(28.37)		9/2 5/2$^+$	M1			0.6×10^{-2}
						E2			3.9×10^{3}
			53.69(9)	0.12(1)	7/2 3/2$^+$	M1			1.3×10^{-2}
						E2			0.9×10^{4}
			82.957(30) [g]	0.005(1) [g]	7/2 5/2$^+$	M1			0.4×10^{-2}
						E2			3.5×10^{3}
			96.224(2) [g]	0.04(1) [g]	5/2 3/2$^+$	E2			0.4×10^{4}
			125.41(6) [g]	0.0018(4) [g]	5/2 5/2$^+$	E2			3.2×10^{3}
146.35	5/2 5/2$^-$	329(8)	74.5390(40) [d]	7.2(2)	7/2 3/2$^+$	E1	0.260	$3.3(1)\times10^{-4}$	8.67×10^{-5}
			117.1628(9) [d]	15.7(5)	5/2 3/2$^+$	E1	0.332	$1.83(7)\times10^{-4}$	1.00×10^{-4}
			146.3462(6) [d]	34(1)	5/2 5/2$^+$	E1	0.195	$2.04(8)\times10^{-4}$	2.50×10^{-4}
148.16	7/2 5/2$^-$	689(34)	(1.81)*	$3.84(34)\times10^{-4}$ [i]	5/2 5/2$^-$	M1	8500	$2.9(3)\times10^{-1}$	1.07×10^{-1}
			76.3507(27) [d]	0.68(2)	7/2 3/2$^+$	E1	0.255	$7.5(4)\times10^{-5}$	1.34×10^{-5}
			118.9721(15) [d]	6.1(2)	5/2 3/2$^+$	E1	0.321	$1.8(1)\times10^{-4}$	8.89×10^{-5}
			148.14(7)	0.62(2)	5/2 5/2$^+$	E1	0.192	$9.3(6)\times10^{-6}$	7.49×10^{-6}
164.52	3/2 3/2$^-$	61(7)	(16.36)*	0.0012(2) [i]	7/2 5/2$^-$	E2	20000	$4.8(10)\times10^{4}$	2.40×10^{4}
			18.17(5) [h]	0.084(14) [i]	5/2 5/2$^-$	M1	155	$4.6(9)\times10^{-2}$	3.23×10^{-2}
			135.3393(5) [d]	37(1)	5/2 3/2$^+$	E1	0.23	$5.4(6)\times10^{-4}$	1.24×10^{-4}
			164.5240(5) [d]	100	3/2 3/2$^+$	E1	0.15	$8.1(10)\times10^{-4}$	7.86×10^{-4}
217.15	5/2 3/2$^-$	30(7)	52.71(5)	0.14(1)	3/2 3/2$^-$	M1	23.5	$1.0(2)\times10^{-1}$	1.22×10^{-1}
			145.46(4)	2.1(1)	7/2 3/2$^+$	E1	0.195	$7.9(19)\times10^{-4}$	8.7×10^{-4}
			187.9669(3) [d]	2.32(7)	5/2 3/2$^+$	E1	0.110	$4.1(10)\times10^{-4}$	5.7×10^{-4}
			217.1519(20) [d]	3.7(1)	3/2 3/2$^+$	E1	0.078	$4.2(10)\times10^{-4}$	2.9×10^{-4}
237.35	7/2 3/2$^-$	$\leq$34	(89.2)*	0.050(16) [i]	7/2 5/2$^-$	M1	5.1	$\geq 2.6\times10^{-2}$	1.51×10^{-2}
			(91.0)*	0.13(2) [i]	5/2 5/2$^-$	M1	4.9	$\geq 6.3\times10^{-2}$	5.90×10^{-2}
			111.4(1)	0.37(3)	9/2 3/2$^+$	E1	0.370	$\geq 1.1\times10^{-3}$	1.80×10^{-3}
			165.0(1)*	0.27(7) [i]	7/2 3/2$^+$	E1	0.145	$\geq 2.4\times10^{-4}$	2.90×10^{-4}
			208.1795(7) [d]	0.61(2)	5/2 3/2$^+$	E1	0.087	$\geq 2.7\times10^{-4}$	3.70×10^{-4}
			237.4(2) [h]	0.6	5/2 5/2$^+$	E1	0.063	$\geq 1.8\times10^{-4}$	1.10×10^{-4}
261.96	1/2 1/2$^+$	15(3)	261.958(4) [d]	38(1)	3/2 3/2$^+$	M1	1.18	$4.5(10)\times10^{-2}$	2.33×10^{-2}
						E2	0.24	$8.2(18)\times10^{3}$	9.21×10^{3}

TABLE. I: *(Continued).*

Initial level [keV]	$I_i K_i^\pi$	$T_{1/2}$ [ps]	E_γ [keV]	I_γ [a]	$I_f K_f^\pi$	$X\lambda$ [a]	α_{TOT} [b]	$B_{exp}(X\lambda)$ [c]	$B_{theor}(X\lambda)$
288.48	3/2 $1/2^+$	16(7)	259.30(7)	9.4(4)	5/2 $3/2^+$	M1	1.22	$4.7(21)\times10^{-2}$	3.80×10^{-2}
			288.5(1)	4	3/2 $3/2^+$	M1	0.90	$1.4(7)\times10^{-2}$	1.21×10^{-2}
303.01	7/2 $7/2^+$	110(17)	154.85(4)	0.37(2)	7/2 $5/2^-$	E1	0.17	$4.5(7)\times10^{-4}$	8.60×10^{-4}
			303.55(7)[h]	0.25(1)	5/2 $5/2^+$	M1	0.78	$3.6(6)\times10^{-3}$	2.11×10^{-3}
317.17	5/2 $1/2^+$	9.0(16)	(28.7)*	0.012(2)[i]	3/2 $1/2^+$	M1	140	$3.3(8)\times10^{-2}$	4.2×10^{-2}
			(55.2)*	0.006(1)[i]	1/2 $1/2^+$	E2	195	$1.1(3)\times10^{4}$	1.5×10^{4}
			99.95(8)	0.22(7)	5/2 $3/2^-$	E1	0.117	$1.6(6)\times10^{-4}$	0.9×10^{-4}
			168.94(5)	0.20(3)	7/2 $5/2^-$	E1	0.140	$3.0(7)\times10^{-5}$	1.7×10^{-5}
			170.8091(24)[d]	0.37(1)	5/2 $5/2^-$	E1	0.136	$5.3(10)\times10^{-5}$	1.7×10^{-5}
			245.3498(11)[d]	10.9(3)	7/2 $3/2^+$	M1	1.45	$3.0(6)\times10^{-2}$	2.5×10^{-2}
						E2	0.31	$4.2(9)\times10^{3}$	3.2×10^{3}
			274.79(5)	1.22(4)	7/2 $5/2^+$	M1	1.02	$1.8(4)\times10^{-3}$	1.2×10^{-3}
						E2	0.27	$3.9(2)\times10^{2}$	2.5×10^{2}
			288.04(4)	4	5/2 $3/2^+$	M1	0.88	$1.1(3)\times10^{-2}$	0.7×10^{-2}
			317.1689(15)[d]	23.4(7)	3/2 $3/2^+$	M1	0.700	$1.9(4)\times10^{-2}$	1.8×10^{-2}
						E2	0.140	$4.1(8)\times10^{3}$	1.2×10^{3}
320.55	5/2 $5/2^+$	10.3(21)	(32.1)*	0.012(2)[i]	3/2 $1/2^+$	M1	105	$3.3(9)\times10^{-2}$	2.5×10^{-2}
			(58.6)*	0.005(1)[i]	1/2 $1/2^+$	E2	145	$9.5(27)\times10^{3}$	5.7×10^{3}
			156.04(9)*	0.31(7)[i]	3/2 $3/2^-$	E1	0.167	$8.3(25)\times10^{-5}$	7.5×10^{-5}
			171.9(2)	0.26(5)	7/2 $5/2^-$	E1	0.135	$5.2(15)\times10^{-5}$	6.1×10^{-5}
			174.1919(20)[d]	0.43(1)	5/2 $5/2^-$	E1	0.130	$8.3(17)\times10^{-5}$	9.5×10^{-5}
			248.74(6)	3.9(10)	7/2 $3/2^+$	M1	1.40	$2.3(8)\times10^{-2}$	1.8×10^{-2}
			278.08(4)	2.55(8)	7/2 $5/2^+$	M1	0.98	$4.7(11)\times10^{-3}$	3.7×10^{-3}
						E2	0.205	$1.1(3)\times10^{3}$	0.9×10^{3}
			291.3561(9)[d]	11.0(3)	5/2 $3/2^+$	M1	0.85	$2.5(5)\times10^{-2}$	2.3×10^{-2}
						E2	0.175	$2.7(6)\times10^{3}$	1.9×10^{3}
			320.5471(13)[d]	5.9(2)	5/2 $5/2^+$	M1	0.68	$5.7(14)\times10^{-3}$	4.9×10^{-3}
						E2	0.135	$1.5(3)\times10^{3}$	1.1×10^{3}
365.81	7/2 $5/2^+$	9(4)	(45.3)*	0.037(7)[i]	5/2 $5/2^+$	M1	38	$8.4(41)\times10^{-2}$	9.7×10^{-2}
			(48.6)*	0.044(9)[i]	5/2 $1/2^+$	M1	31	$8.1(40)\times10^{-2}$	5.6×10^{-2}
			217.6(1)	0.19(5)	7/2 $5/2^-$	E1	0.078	$4.3(22)\times10^{-5}$	5.6×10^{-5}
			219.55(4)	0.53(2)	5/2 $5/2^-$	E1	0.076	$1.2(5)\times10^{-4}$	1.8×10^{-4}
			240.5(1)	1.17(3)	9/2 $3/2^+$	M1	1.50	$1.1(5)\times10^{-2}$	0.9×10^{-2}
						E2	0.32	$1.7(8)\times10^{3}$	0.7×10^{3}
			268.6747(21)[d]	1.04(3)	9/2 $5/2^+$	M1	1.10	$7.2(33)\times10^{-3}$	6.7×10^{-3}
						E2	0.23	$8.2(38)\times10^{2}$	6.5×10^{2}
			293.995(9)[d]	0.53(2)	7/2 $3/2^+$	M1	0.84	$4.4(20)\times10^{-3}$	3.9×10^{-3}
			323.3806(14)[d]	3.3(1)	7/2 $5/2^+$	M1	0.66	$5.4(25)\times10^{-3}$	7.01×10^{-3}
						E2	0.128	$2.1(9)\times10^{3}$	1.2×10^{3}
			336.6195(16)[d]	2.35(7)	5/2 $3/2^+$	M1	0.60	$3.7(19)\times10^{-3}$	2.9×10^{-3}
						E2	0.118	$1.2(5)\times10^{3}$	0.9×10^{3}
			365.75(4)	3.2(1)	5/2 $5/2^+$	M1	0.48	$1.4(6)\times10^{-2}$	1.1×10^{-2}
423.95	1/2 $1/2^-$	190(8)	135.55(7)*	1.1(2)[i]	3/2 $1/2^+$	E1	0.23	$1.8(3)\times10^{-4}$	1.6×10^{-4}
			162.01(5)	0.64(2)	1/2 $1/2^+$	E1	0.155	$6.1(3)\times10^{-5}$	5.5×10^{-5}
			259.40(3)	1.6(3)	3/2 $3/2^-$	M1	1.22	$3.4(6)\times10^{-3}$	2.9×10^{-3}
425.30	3/2 $1/2^-$	290(48)	163.35(5)	0.4	1/2 $1/2^+$	E1	0.15	$6.6(20)\times10^{-5}$	5.9×10^{-5}
			277.21(6)	0.31(4)[i]	7/2 $5/2^-$	E2	0.21	$1.8(4)\times10^{2}$	1.1×10^{2}
			278.7(1)*	0.49(7)[i]	5/2 $5/2^-$	M1	0.98	$1.5(3)\times10^{-3}$	0.9×10^{-3}
			425.36(5)[h]	0.27(1)	3/2 $3/2^+$	E1	0.018	$2.5(4)\times10^{-6}$	2.1×10^{-6}

TABLE. I: *(Continued).*

Initial level [keV]	$I_i K_i^\pi$	$T_{1/2}$ [ps]	E_γ [keV]	I_γ [a]	$I_f K_f^\pi$	$X\lambda$ [a]	α_{TOT} [b]	$B_{exp}(X\lambda)$ [c]	$B_{theor}(X\lambda)$
478.58	5/2 1/2$^-$	≤16	157.88(9)	0.8(2)	5/2 5/2$^+$	E1	0.165	$\geq 1.5\times10^{-4}$	1.1×10^{-4}
			189.6(1)	0.09(1)	3/2 1/2$^+$	E1	0.11	$\geq 9.8\times10^{-6}$	2.5×10^{-6}
			241.18(9)*	0.55(9)[i]	7/2 3/2$^-$	M1	1.48	$\geq 2.6\times10^{-3}$	1.2×10^{-3}
			261.80(9)*	0.58(8)[i]	5/2 3/2$^-$	M1	1.18	$\geq 2.2\times10^{-3}$	1.9×10^{-3}
			314.12(5)*	0.78(10)[i]	3/2 3/2$^-$	M1	0.72	$\geq 1.7\times10^{-3}$	1.2×10^{-3}
			330.54(4)	0.49(2)	7/2 5/2$^-$	M1	0.63	$\geq 9.1\times10^{-4}$	7.6×10^{-4}
			332.52(4)[h]	0.09(1)	5/2 5/2$^-$	M1	0.63	$\geq 1.6\times10^{-4}$	0.9×10^{-4}
			406.53(8)*	3.5(6)[i]	7/2 3/2$^+$	E1	0.0195	$\geq 3.9\times10^{-5}$	1.7×10^{-5}
			436.20(4)[h]	5.6(2)	7/2 5/2$^+$	E1	0.017	$\geq 5.0\times10^{-5}$	3.8×10^{-5}
			449.17(9)	3.7(6)[i]	5/2 3/2$^+$	E1	0.0155	$\geq 3.0\times10^{-5}$	1.7×10^{-5}
			478.64(4)[h]	17.5(5)	5/2 5/2$^+$	E1	0.014	$\geq 1.2\times10^{-4}$	0.8×10^{-4}

[a] γ-ray intensities and δ^2(E2/M1) mixing ratios are from Ref. [15] except when noted otherwise.
[b] Total internal conversion coefficients for transitions with energies above 21 keV are from Ref. [21], while for transitions with lower energies from Ref. [22] .
[c] in the units e^2fm^2 for E1 transitions, e^2fm^4 for E2 transitions and μ_N^2 for M1 transitions.
[d] γ ray energy adopted from Ref. [2].
[e] Lifetimes of the 42.3 and 97.1 keV levels are from Ref. [17].
[f] Individual intensities of the 42-keV doublet are deduced from $\gamma\gamma$ coincidence results and the total intensity from Ref. [15].
[g] δ^2(E2/M1) for the 42.34 keV γ-ray and data concerning γ-transitions de-exciting the 97.14 and 125.51 keV levels are from Ref. [23]. Intensities of γ-transitions were re-normalized to the units used in Ref. [15].
[h] from Ref. [15].
[i] γ-ray intensity determined in this work.

TABLE II: New γ-lines in ^{229}Th not listed in Table I.

E_γ [keV]	I_γ	Initial level [keV]
24.8(1)		661.6
69.1(2)		638.6
83.9(2)		689.0
84.8(1)		654.0
156.3(1)	1.6(6)	605.3
161.46(8)	0.53(10)	449.7
203.47(6)	0.94(12)	569.3
343.3(1)	0.18(4)	605.3
526.4(4)	2.1(8)	569.3

estimated by extrapolation of values listed in Ref. [22].

IV. DISCUSSION

A. Single quasiparticle configurations in ^{229}Th

The occurrence of strong octupole correlations in odd-A nuclei is manifested by the presence of parity doublet bands and enhanced E1 transitions between members of these bands. This effect persists in the ocupole soft nuclei where significant octupole coupling may exist between selected close-lying bands of opposite parity. For this reason these bands are labelled *parity partner bands* [24] (see also discussion in Sec. IV C).

In the case of parity doublet $K^\pi=1/2^\pm$ bands the decoupling parameters are expected to be of equal magnitudes and opposite signs. According to the single quasiparticle calculations performed by Ćwiok and Nazarewicz [25, 26] for ^{229}Th, one expects nine single-particle states below 1 MeV: three states with K=1/2, two with K=3/2, three with K=5/2 and one state with K=7/2. Our single-particle calculations (see Sec. IV E) predict one more K=7/2 level at a similar, although slightly higher, excitation energy.

Configuration assignment to the five rotational bands built on the K=3/2 and K=5/2 states (see Fig. 7) has already been made in the earlier studies [8, 13, 15, 27]. Furthermore, the 1/2[631] and 1/2[501] configurations have been assigned to the rotational bands built on two K=1/2 levels at the energies of 262.0 and 535.7 keV, respectively. Recently, in the α-decay study [16] the 317.2 keV level has been proposed as the $5/2^+$ member to the first K=1/2 band. Decoupling parameter a for this band is found to be equal to 0.21 and can be compared to the theoretical value of 0.30 predicted by Leander and

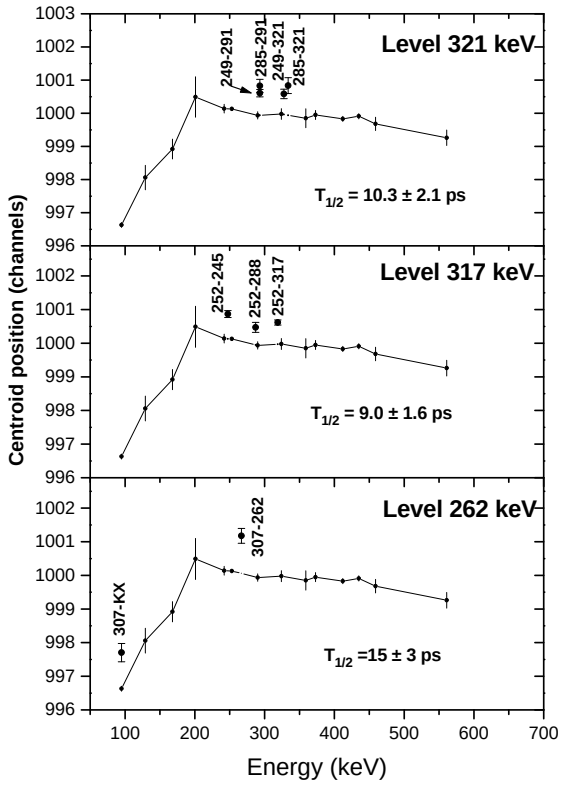

FIG. 6: Determination of half-lives for the 262.0, 317.2 and 320.6 keV levels by centroid shift technique. Each figure shows the reference curve (solid line) and centroid positions of time-delayed spectra marked by the energies (in keV) of γ-ray gates in the Ge and BaF_2 detectors. The shift of the time-delayed centroid from the reference curve gives the mean-life of the level (calibration 20.00(6) ps/ch); see text for details.

Chen [28] and to 0.285 obtained in the calculations of Sec. IV C. The B(E2) value of $1.1(3)\times10^4$ e^2fm^4 deduced from our data for the 55.2 keV intra-band transition gives for this band the quadrupole moment of 7.4(9) eb and the quadrupole deformation parameter β_2=0.20. The latter value is close to the β_2 equilibrium deformation of 0.18 obtained in our calculations of Sec. IV E for the configuration with 1/2[631] as the main component. The magnetic $|g_K - g_R|(1-b)$ factor determined for this band from the B(M1) value of the 28.7 keV transition is equal to 1.18(14) (see Table IV).

The only new information obtained in this work for the second K=1/2 band built on the 535.7 keV level is the theoretical value of the decoupling parameter a=0.27, predicted in our calculations of Sec. IV C.

Based on our new data, we propose the 424.0 keV $(1/2^-)$ level as the head of the third K=1/2 band with the 425.3 keV state as the $3/2^-$ band member. The proposed interpretation conflicts with the M1 multipolarity given [15] to the 425.4 keV transition. We note, however, that the 425.4 keV transition was assigned to this level based on energy match and not due to $\gamma\gamma$ coincidences, thus its assignment to this state is not firm. On the other hand, if the parity assignment to the 425.3 keV level would be positive, then the 277.2 keV transition to the $7/2^-$ state would be of M2 type, which is very unlikely. For the $5/2^-$ member of this band we propose the 478.6 keV level. The decoupling parameter a obtained for this band is equal to -0.92 and may be compared to the theoretical value of -1.4 obtained from calculations of Sec. IV C. These calculations give 1/2[770] as the main component of the intrinsic wave function for this band. In view of the potential energy calculations from Sec. IV E intrinsic state with this wave function component is predicted to be octupole deformed and this band could be a candidate for the negative parity member of the K = 1/2 parity doublet bands.

For the 478.6 keV level we prefer the $5/2^-$ assignment proposed above, instead of $7/2^-$ given in Ref. [15] since then the 189.6 keV transition would become unreasonably fast M2 line. Moreover, we do not observe neither the 315.39 nor the 381.54 keV transition to de-excite this state, as proposed in [16].

The 303.0 keV level has been tentatively interpreted in Ref. [16] as head of the $K^\pi=7/2^+$ band. This band may originate from the 7/2[613] configuration. Second K=7/2 configuration which originates from the 7/2[743] orbital is predicted to be octupole deformed (see Sec. IV E). We tentatively propose the 465.4 keV level as one of the parity doublet band-heads assigned to this configuration. This level is populated in the α-decay of ^{233}U [16] and de-excites to the $7/2^+$ state at 303.0 keV via 162.5 keV transition.

TABLE III: Structure of the intrinsic states in ^{229}Th calculated within the QPPM model. The band labels are the same as in Fig. 7.

Band Label	Structure of the wave function
A	$5/2[633](84\%)+(5/2[752]+Q_{30}^+)(4\%)$ $+(5/2[503]+Q_{30}^+)(2\%)$
A'	$5/2[622](85\%)+5/2[633](1\%)+(5/2[752]+Q_{30}^+)(5\%)$
B	$3/2[631](43\%)+3/2[642](31\%)+(3/2[761]+Q_{30}^+)(12\%)$
C	$1/2[631](57\%)+1/2[640](11\%)+1/2[651](7\%)$ $+(1/2[770]+Q_{30}^+)(8\%)+1/2[501]+Q_{30}^+)(2\%)$
D	$3/2[642](43\%)+3/2[631](28\%)+(3/2[761]+Q_{30}^+)(19\%)$ $+(3/2[501]+Q_{30}^+)(3\%)$
E	$7/2[613](39\%)+7/2[624](37\%)+(7/2[743]+Q_{30}^+)(12\%)$
a	$5/2[752](83\%)+5/2[503](1\%)+(5/2[633]+Q_{30}^+)(11\%)$
b	$3/2[761](80\%)+(3/2[642]+Q_{30}^+)(14\%)$ $+(3/2[651]+Q_{30}^+)(2\%)$
c	$1/2[501](77\%)+1/2[770](1\%)+(1/2[651]+Q_{30}^+)(9\%)$ $+(1/2[640]+Q_{30}^+)(5\%)+(1/2[660]+Q_{30}^+)(3\%)$
c'	$1/2[770](70\%)+1/2[501](8.2\%)+(1/2[640]+Q_{30}^+)(9.3\%)$
e	$7/2[743](75\%)+(7/2[624]+Q_{30}^+)(18\%)$

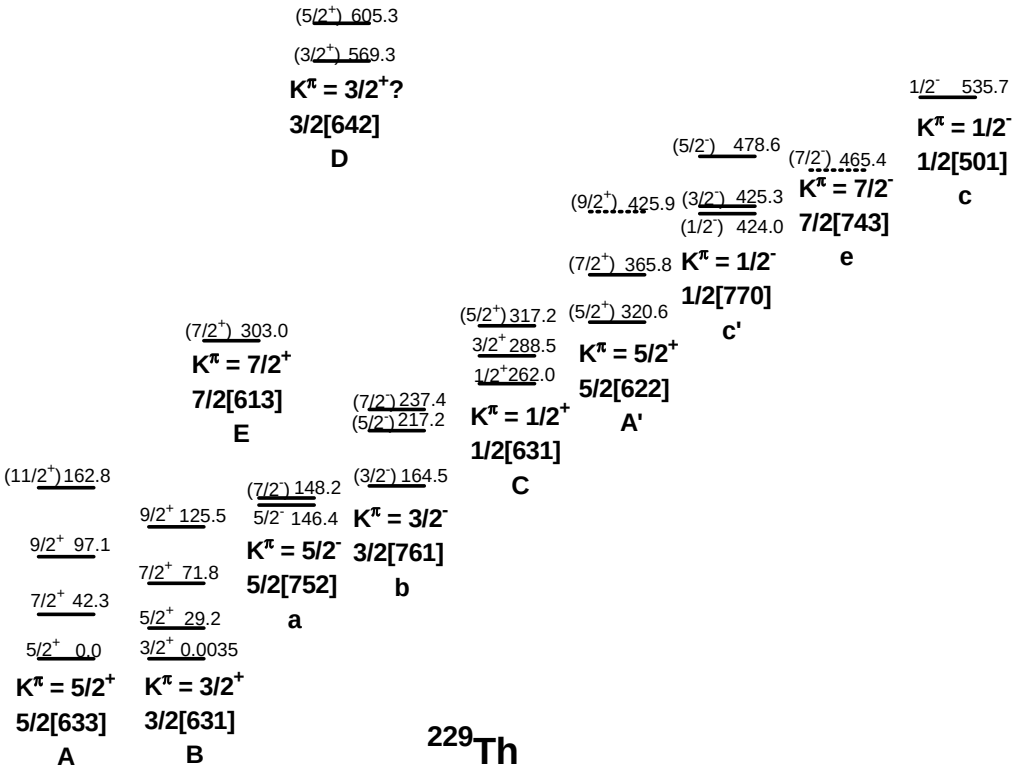

FIG. 7: Experimental levels in ^{229}Th grouped into rotational bands. Dashed lines represent levels populated in the α-decay [8, 9, 16]. Each band is labelled by the dominant single-quasiparticle component of the wave function as obtained in the calculations in Section IV C. The structure of the intrinsic states forming the base for each rotational band is given in Table III. The pairs of bands labelled by the same small and capital letters are interpreted as parity partner bands.

TABLE IV: Magnetic g factors for the rotational bands in ^{229}Th.

Band K^π	E_i [keV]	E_γ [keV]	I_i	$\lvert g_K - g_R \rvert$
$5/2^+$	42.34	42.34	$7/2^+$	0.24(3)[a]
	97.14	54.699	$9/2^+$	0.14(2)[a]
$5/2^-$	148.16	1.81	$7/2^-$	0.95(5)
$3/2^-$	217.15	52.71	$5/2^-$	0.84(10)
$1/2^+$	317.17	28.7	$5/2^+$	1.18(14)[b]
$5/2^+$	365.81	45.3	$7/2^+$	0.51(12)

[a] from data in Ref. [23].
[b] $|g_K - g_R|(1-b)$ where b is the magnetic decoupling parameter.

Table V shows a comparison of the experimental branching ratios for the E1 and M1 transitions to the theoretical intensity ratios given by the Alaga's rule [29]. A good agreement is observed only for the E1 transitions connecting levels from the K^π=$3/2^-$ band at 164.5 keV with levels of the K^π=$3/2^+$ band at 0.0035 keV (see lower part of Table V). This confirms the K^π assignment for these bands. For other bands a clear deviation from the Alaga rule is observed suggesting that most of the bands in ^{229}Th are strongly Coriolis mixed.

Theoretical branching ratios for the Coriolis coupled bands are described by the Mikhailov rule [30]. In practise, this rule can be applied to experimental data only when $|K_f - K_i| \geq \lambda$ and when the degree of K-forbiddennes n=0. Only in this case the Mikhailov rule takes a simple form:

$$B(X\lambda) = M_{if}^2 \langle I_i K_i \lambda (K_f - K_i) | I_f K_f \rangle^2 \times [1 + [I_f(I_f+1) - I_i(I_i+1)]]^2 a_M^2$$

with one free parameter a_M. As can be seen in the upper part of Table V this rule nicely reproduces branching ratios for the E1 transitions between K^π=$5/2^-$ and K^π=$3/2^+$ bands with band heads at 146.4 keV and 0.0035 keV, respectively. For this comparison, the value

of a_M was set to 0.323.

B. B(E1) rates

A common property of nuclei with strong octupole correlations are enhanced E1 transitions. A significant number of reduced transition probabilities B(E1) listed in column 9 of Table I is moderately fast, of the order of 10^{-4} e^2fm^2, while typical B(E1) values for nuclei from non-octupole collective regions are much slower, below 10^{-5} e^2fm^2. In particular, the E1 transitions connecting members of the $K^\pi=3/2^\pm$ bands with band heads at 0.0035 and 164.5 keV have B(E1) values higher than 1.8×10^{-4} e^2fm^2. Evidently, these bands constitute a pair of parity partner bands. The E1 transitions between parity partner bands with $K^\pi=5/2^\pm$ and $1/2^\pm$ are significantly less enhanced. No clear difference is observed between E1 transitions connecting the parity partner bands (intra-band transitions) and those connecting opposite parity bands with different K (inter-band transitions). The B(E1) values for many E1 inter-band transitions with $|\Delta K| = 1$ are of the order 10^{-4} e^2fm^2. This provides another indication that rotational bands in ^{229}Th are strongly mixed since mixing would enhance the inter-band transitions to the values comparable to those for intra-band.

A generally adopted way of comparison of the E1 strength over a wider range of nuclei is offered by the intrinsic electric dipole moment, $|D_0|$, which removes the spin dependence affecting the B(E1) rates. Assuming a strong-coupling limit and an axial shape of the nucleus, the electric dipole moment, $|D_0|$, is defined (for $K \neq 1/2$) via the rotational formula:

$$B(E1) = \frac{3}{4\pi} D_0^2 \langle I_i K 10 | I_f K \rangle^2.$$

It should be emphasized that the $|D_0|$ moment remains a convenient parameter for the inter-comparison even though this rotational formula may not be strictly applicable to such an octupole transitional nucleus as ^{229}Th.

Table VI provides the $|D_0|$ moments deduced from the B(E1) values given in Table I for the parity partner bands in ^{229}Th. The highest $|D_0|$ values of 0.077(3) efm (on the average) are obtained for the E1 transitions connecting the $K^\pi=3/2^\pm$ bands. Much smaller average $|D_0|$ values of 0.024(5) and 0.029(1) efm are deduced for the $K^\pi=5/2^\pm$ and $1/2^\pm$ bands, respectively. Figure 8 shows a comparison of the $|D_0|$ values from Table VI to those for the $K^\pi=1/2^\pm$, $3/2^\pm$ and $5/2^\pm$ parity doublet or parity partner bands in other odd-A isotopes of Th. They may also be compared to the average values of $|D_0| = 0.10$ efm and ≥ 0.11 efm for the $K^\pi=3/2^\pm$ and $1/2^\pm$ bands in ^{227}Ra [31], the isotone of ^{229}Th, respectively and to the $|D_0|$ values for the $K^\pi=0^\pm$ bands in ^{228}Th and ^{230}Th, where $|D_0| = 0.121(3)$ efm and 0.053(2) efm, respectively, were determined from the B(E1)/B(E2) ratios measured in [32] and the Q_0 values taken from [33]. One may conclude, that the $|D_0|$ moments in ^{229}Th follow the smoothly decreasing trend of these values when moving from the center of the octupole collective region to the heavier reflection-symmetric thorium isotopes. Moreover, the difference between the intra- and inter-band E1 transitions diminishes with the decreasing strength of octupole correlations.

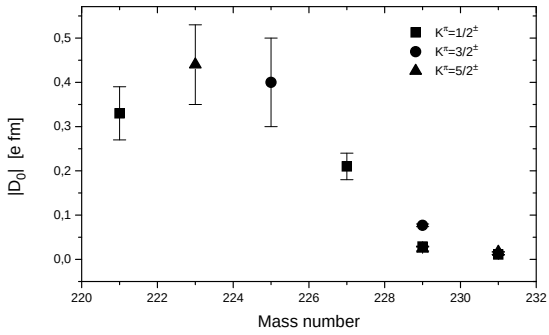

FIG. 8: Electric dipole moments for the $K^\pi=1/2^\pm$, $3/2^\pm$ and $5/2^\pm$ parity doublet or parity partner bands in the odd-A thorium isotopes. Experimental data are from Refs. [24, 34–37] and from this work.

C. Quasiparticle-plus-phonon model calculations

The experimental B(E1) rates, as well as rates for the E2 and M1 transitions, are compared to the results of the quasiparticle-plus-phonon model (QPPM) calculations in columns 9 and 10 of Table I, respectively.

In the strong correlation limit octupole correlations lead to a stable octupole deformation of the nuclear mean field (nonzero value of the intrinsic dipole moment $|D_0|$). In the weak octupole correlation limit these correlations are not strong enough to form stable octupole deformation but are sufficiently strong to shift octupole vibrations in even-even nuclei to very low excitation energies. In the corresponding odd-A nuclei these correlations manifest themselves by relatively large octupole vibrational components in the lowest excited states. The best description of this situation is provided by the quasiparticle-plus-phonon model (see Refs. [24, 25, 31, 38] and citations therein) where the lowest intrinsic states in odd-A nuclei are understood as the linear combinations of quasiparticle and quasiparticle-plus-phonon components. In such a way the QPPM takes into account an odd quasiparticle and vibrating even-even core. For nuclei from the region of weak octupole correlations the lowest even-even core vibrations have an octupole character.

The QPPM Hamiltonian consists of the intrinsic and rotational parts (with inclusion of Coriolis mixing). The intrinsic part of the Hamiltonian describes intrinsic states

TABLE V: Comparison of experimentally obtained branching ratios for the E1 transitions in ^{229}Th to the Alaga and Mikhailov rules.

Initial level	I_i^π K_i	I_f^π K_f	E_γ	Reduced branching ratios		
				exp	theory	
[keV]			[keV]		Alaga	Mikhailov[a]
146.35	$5/2^-$ 5/2	$5/2^+$ 3/2	117.16	1	1	1
		$7/2^+$ 3/2	74.54	1.78(8)	0.17	1.78
148.16	$7/2^-$ 5/2	$5/2^+$ 3/2	118.97	1	1	1
		$7/2^+$ 3/2	76.35	0.42(2)	0.71	0.45
164.52	$3/2^-$ 3/2	$3/2^+$ 3/2	164.52	1	1	
		$5/2^+$ 3/2	135.34	0.66(3)	0.67	
217.15	$5/2^-$ 3/2	$3/2^+$ 3/2	217.15	1	1	
		$5/2^+$ 3/2	187.97	0.97(4)	0.96	
		$7/2^+$ 3/2	145.46	1.89(10)	1.79	
237.35	$7/2^-$ 3/2	$5/2^+$ 3/2	208.18	1	1	
		$7/2^+$ 3/2	165.0	0.9(2)	0.40	
		$9/2^+$ 3/2	111.4	4.0(4)	1.40	

[a]obtained using parameter a_M=0.323

TABLE VI: Intrinsic dipole moments, $|D_0|$, for the E1 transitions in ^{229}Th.

E_i	$I_i^\pi K_i$	E_γ	$I_f^\pi K_f$	$\|D_0\|$
[keV]		[keV]		[efm]
146.35	$5/2^-$ 5/2	146.35	$5/2^+$ 5/2	0.0345(7)
148.16	$7/2^-$ 5/2	148.14	$5/2^+$ 5/2	0.0135(4)
164.52	$3/2^-$ 3/2	135.34	$5/2^+$ 3/2	0.075(4)
		164.52	$3/2^+$ 3/2	0.075(5)
217.15	$5/2^-$ 3/2	145.46	$7/2^+$ 3/2	0.084(10)
		187.97	$5/2^+$ 3/2	0.081(10)
		217.15	$3/2^+$ 3/2	0.081(10)
237.35	$7/2^-$ 3/2	111.4	$9/2^+$ 3/2	$\geq$0.095
		165.0	$7/2^+$ 3/2	$\geq$0.084
		208.18	$5/2^+$ 3/2	$\geq$0.057
320.55	$5/2^+$ 5/2	171.9	$7/2^-$ 5/2	0.028(4)
		174.19	$5/2^-$ 5/2	0.022(2)
365.81	$7/2^+$ 5/2	217.6	$7/2^-$ 5/2	0.021(6)
		219.55	$5/2^-$ 5/2	0.048(11)
423.95	$1/2^-$ 1/2	135.55	$3/2^+$ 1/2	0.034(3)[a]
		162.01	$1/2^+$ 1/2	0.028(1)[a]
425.30	$3/2^-$ 1/2	163.55	$1/2^+$ 1/2	0.029(4)[a]
478.58	$5/2^-$ 1/2	189.6	$3/2^+$ 1/2	$\geq$0.010[a]

[a]with D_1 term neglected

of a nucleus while the rotational part creates rotational bands build on top of those states. The rotational bands are mixed by the Coriolis interaction. In our calculations the intrinsic Hamiltonian involves phenomenological mean field of the Nilsson type (with the axial quadrupole and hexadecapole deformations), monopole pairing residual interactions, and long-range residual interactions in the quadrupole-quadrupole and octupole-octupole form (for details see e.g. [24, 40]). Appropriate choice of the model parameters gives a good agreement between the calculated energy spectrum and the experimental one as shown in Fig. 7 (see also Figs. 8 and 9 in Ref. [15]). Contributions from dominant quasiparticle and quasiparticle-plus-phonon components into each intrinsic state are listed in Table III. It can be seen that octupole phonons play a significant role in this nucleus. Moreover, one can recognize some kind of a parity-doublet structure among the bands in the sense that we can indentify two bands, one of positive parity (labelled with a capital letter) and corresponding negative parity partner (labelled with a corresponding lower case letter). In each such pair of bands (e.g.: A-a or B-b etc.), which we define as *parity partner bands*, the dominating single-quasiparticle component of one band forms the dominating collective quasiparticle-plus-octupole-phonon (Q_{30}^+) component of the second band, and vice versa. In such a way the QPPM reflects the parity doublet structure which is a characteristic feature of strong octupole correlations.

One observes a very good agreement between the experimental reduced transition probabilities $B_{exp}(X\lambda)$ and the theoretical values $B_{theor}(X\lambda)$ calculated in the framework of the QPPM with the Coriolis mixing (see Table I). The QPPM approach provides a good description of the reduced probabilities even in the case of inter-band transitions, which is due to the inclusion of octupole correlations in the residual interactions and by taking into account the Coriolis mixing. The drawback of the QPPM model in the form applied here is that it does not involve the residual interactions entirely and the vibrations of the even-even core are treated only on the RPA harmonic level (anharmonic effects are neglected).

D. Half-life of the low-energy $3/2^+$ isomer

For the M1 γ-ray transition connecting the low-energy $3/2^+$ level and the $5/2^+$ ground state, the QPPM calculations yield the reduced probability B(M1) = 0.025 μ_N^2 (see Table I). The half-life of this transition, expressed in hours, can be obtained from the relation $T_{1/2} = 10.95h/E_\gamma^3 B(M1)$, where E_γ is given in eV. The assumption of $E_\gamma = (3.5 \pm 1.0)$ eV [2] leads to $T_{1/2} = 10^{+18}_{-5}$ hours, while by using the recently re-evaluated energy value of $E_\gamma = (5.5 \pm 1.0)$ eV [3] one obtains $T_{1/2} = 2.6^{+2.2}_{-1.0}$ hours. A comparison of model predictions to an experimental half-life of the isomer, when a reliable $T_{1/2}$ value will be available, would require a correction for the effect of an electronic bridge [41], which is an additional decay channel for the isomer.

Within our experimental approach, the half-life measurement of the isomeric state was not possible. Earlier, two groups attempted to determine this half-life using radiochemical and α-spectroscopy techniques. Browne et al. [6] separated the activity of ^{229}Th, and presumably of ^{229m}Th, from a sample of ^{233}U, and searched for a short-lived α-ray component originating from the decay of the isomer. The result of that experiment was negative. It has been concluded that the ^{229m}Th half-life must be either shorter than 6 h or longer than 20 days. This conclusion is in conflict with the results reported by Mitsugashira et al. [42]. In the latter work, the ^{229m}Th activity was sought by producing it through the (γ,n) reaction on a ^{230}Th target. The α-spectrum of the chemically separated thorium fraction was measured as a function of time. The half-life observed for the component at about 5 MeV (the energy of the α-radiation expected for ^{229m}Th) was found to be 13.9 $\pm$ 3.0 h. This value assigned to the isomer is compatible with our predictions based on the isomer energy of 3.5 $\pm$ 1.0 eV. However, in view of the disagreement between the results obtained by the two groups, further efforts to measure the half-life of the isomer are obviously needed. In Ref. [42], a study of the α-decay of ^{229m}Th after β-decay of ^{229}Ac has been suggested. For a stringent test of the model predictions, also a more accurate determination of the isomer energy would be required.

E. Potential energy surfaces

Octupole correlations can be accounted for in an alternative approach by including octupole deformation parameter, β_3, into the model calculations.

We have calculated band head energies and potential energy surfaces on the (β_2,β_3) plane for the lowest quasi-particle configurations in ^{229}Th. The calculations were performed using the Strutinsky method, in which macrosopic energy contribution is obtained using the liquid-drop formula with the surface diffuseness term [43], whereas shell correction is calculated using the axially-deformed Woods-Saxon potential with the universal set of parameters [44]. Potential energy surfaces for specific configurations (see Fig. 9) have been obtained by blocking the odd neutron in state with a given K and by minimization of total energy with respect to the shape parameters $\beta_4 - \beta_6$. These calculations show that for all considered configurations quadrupole deformation β_2 is within the range of $0.15 - 0.20$. Moreover, they show that the ^{229}Th nucleus is reflection-symmetric or slightly octupole-soft in all single quasi-particle configurations with spins 3/2 and 5/2. Distinct octupole softness is predicted for two K = 1/2 configurations with the dominating 1/2[631] and 1/2[501] single-particle components. Octupole deformation of $\beta_3 \sim 0.12$ is expected only for the K = 7/2 configuration with the main component 7/2[743] and for the K = 1/2 configuration with 1/2[770] as the main component. However, the octupole minima are not very deep and octupole barrier heights are lower than 0.5 MeV.

These calculations do not explain why enhanced E1 transitions are observed for the $K^\pi = 3/2^\pm$ configurations and why such transitions are weaker for the $K^\pi = 5/2^\pm$ and $K^\pi = 1/2^\pm$ bands.

Potential energy calculations performed for two odd-A neighbors of ^{229}Th show that the ^{227}Th nucleus is reflection-asymmetric in all but one lowest configuration while no octupole deformation is predicted for ^{231}Th. Only two configurations in the latter nucleus are foreseen to be octupole soft. Thus one concludes that ^{229}Th lies at the border of the actinide octupole collective region and coexistence of the reflection-asymmetric and reflection-symmetric shapes is predicted in this nucleus.

V. SUMMARY

The Advanced Time-Delayed $\beta\gamma\gamma$(t) method has been used to measure half-lives of 14 excited states in ^{229}Th. Reduced transition probabilities were obtained for more than 70 transitions. Twenty-seven new γ-lines have been introduced into the decay scheme of ^{229}Ac. Enhanced E1 transitions are observed between the $K^\pi = 3/2^\pm$ bands.

A good agreement between experimental transition probabilities and results of the QPPM calculations implies octupole-vibrational nature of the lowest configurations in ^{229}Th and strong Coriolis coupling of the $K^\pi = 3/2^-$ and $K^\pi = 1/2^-$ bands. It indicates that one can describe the low-lying states in ^{229}Th without the stable octupole deformation in the mean field. The octupole softness is also confirmed by the potential energy surface calculations. A non zero octupole deformation is foreseen only for one K=1/2 and one K=7/2 state lying at higher excitation energies.

Our results confirm the location of ^{229}Th nucleus at the border of the collective octupole region in actinides where the interplay takes place between reflection-symmetric and asymmetric configurations.

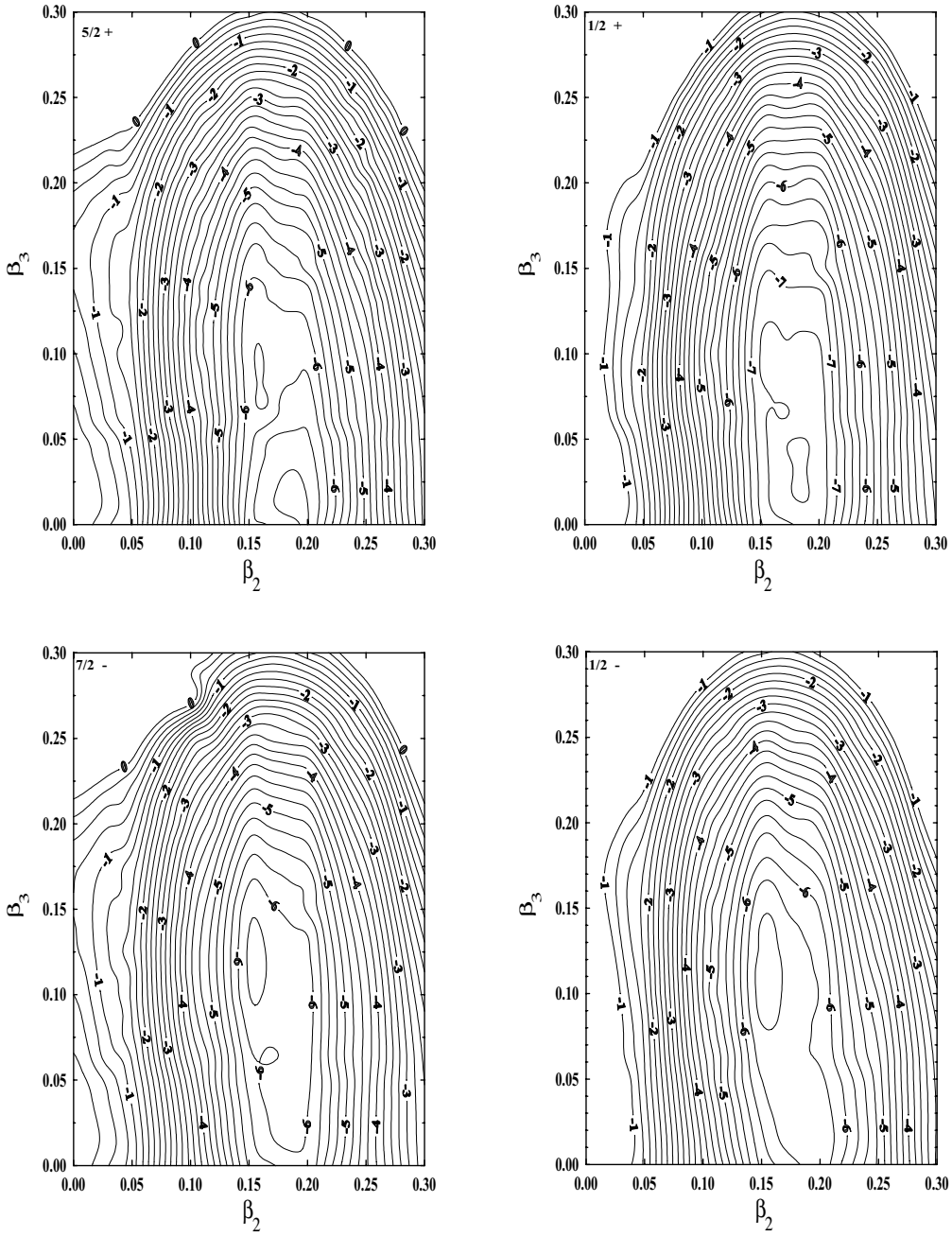

FIG. 9: Potential energy surfaces calculated for the $K^{\pi} = 5/2^{+}$ ground state (upper left panel), for two K = 1/2 bands with band heads at 262.0 and 424.0 keV (upper right and lower right panels, respectively) and for the K = 7/2 band with band head at 465.4 keV (lower left panel). The energy distance between the contour lines is equal to 0.25 MeV.

Acknowledgments

This work has been supported in part by the grant No. 1 P03B 059 27 from the Polish Committee for Scientific Research (KBN) (for theoretical calculations), the Swedish Research Council, the research plan MSM0021620834 provided by the Ministry of Education of the Czech Republic and the Spanish CICYT under project number FPA2002-04181-C04-02. Support by the European Commission through the HPRI-CT-1999-00018 project and by the ISOLDE Collaboration are also acknowledged. Fast timing detectors and electronics have been provided by the Fast Timing Pool of Electronics. One of us (E.R.) would like to thank the OSIRIS group for their generous hospitality and for financial support during her stay in Studsvik.

[1] G.A. Leander and R.K. Sheline, Nucl. Phys. **A413**, 375 (1984).
[2] R.G. Helmer, C.W. Reich, Phys. Rev. C **49**, 1845 (1994).
[3] Z.O. Guimaraes-Filho, O. Helene, Phys. Rev. C **71**, 044303 (2005).
[4] F.F. Karpeshin, S. Wycech, I.M. Band, M.B. Trzhaskovskaya, M. Pfützner, and J. Żylicz, Phys. Rev. C **57**, 3085 (1998).
[5] E.V. Tkalya, A.N. Zherikhin, and V.I. Zhudov, Phys. Rev. C **61**, 064308 (2000).
[6] E. Browne, E.B. Norman, R.D. Canaan, D.C. Glasgow, J.M. Keller, and J.P. Young, Phys. Rev. C **64**, 014311 (2001).
[7] K. Pachucki, S. Wycech, J. Żylicz, and M. Pfützner, Phys. Rev. C **64**, 064301 (2001).
[8] L.A. Kroger, and C.W. Reich, Nucl. Phys. **A259**, 29 (1976).
[9] M.J. Canty, R.D. Connnor, D.A. Dohan and B. Pople, J. Phys. **G3**, 421 (1977).
[10] K. Chayawattanangkur, G. Herrmann, and N. Trautmann, J. Inorg. Nucl. Chem. **35**, 3061 (1973).
[11] I. Ahmad, J.E. Gindler, R.R. Betts, and R.R. Chasman, Phys. Rev. Lett. **49**, 1758 (1982).
[12] Y.A. Ellis, Nucl. Data Sheets **6**, 257 (1971).
[13] D.G.. Burke, P.E. Garret, Tao Qu, and R.A. Naumann, Phys. Rev. C **42**, R499 (1990).
[14] C.E. Bemis, F.K. McGowan, J.L.C. Ford, W.T. Milner, R.L. Robinson, P.H. Stelson, G.A. Leander, and C.W. Reich, Physica Scripta **38**, 657 (1988).
[15] K. Gulda, W. Kurcewicz, A.J. Aas, M.J.G. Borge, D.G. Burke, B. Fogelberg, I.S. Grant, E. Hagebø, N. Kaffrell, J. Kvasil, G. Løvhøiden, H. Mach, A. Mackova, T. Martinez, G. Nyman, B. Rubio, J.L. Tain, O. Tengblad, T.F. Thorsteinsen, and the ISOLDE Collaboration, Nucl. Phys. **A703**, 45 (2002).
[16] V. Barci, G. Ardisson, G. Barci-Funel, B. Weiss, O. El Samad, and R.K. Sheline, Phys. Rev. C **68**, 034329 (2003).
[17] H. Ton, S. Roodbergen, J. Brasz and J. Blok Nucl. Phys. **A155**, 245 (1970).
[18] H. Mach, R.L.Gil and M. Moszyński Nucl. Instrum. Methods A **280**, 49 (1989).
[19] M. Moszyński and H. Mach, Nucl. Instrum. Methods A **277**, 407 (1989).
[20] H. Mach, F.K. Wohn, G. Molnár, K. Sistemich, John C. Hill, M. Moszyński, R.L. Gill, W. Krips, and D.S. Brenner, Nucl. Phys. **A523**, 197 (1991).
[21] I.M. Band, M.B. Trzhaskovskaya, C.W. Nestor, P.O.Tikkanen and S. Raman, At. Data Nucl. Data Tables. **81**, 1 (2002).
[22] F. Rösel, H.M. Fries, K. Alder, and H.C. Pauli, At. Data Nucl. Data Tables. **21**, 291 (1978).
[23] R.B. Firestone, S.Y.F. Chu and C.M. Baglin, Table of Isotopes CD-ROM, 8^{th} Edition: 1999 Update, Wiley-Interscience.
[24] A.J. Aas, H. Mach, J. Kvasil, M.J.G. Borge, B. Fogelberg, I.S. Grant, K. Gulda, E. Hagebø, P. Hoff, W. Kurcewicz, A. Lindroth, G. Løvhøiden, A. Mackova, T. Martínez, B. Rubio, M. Sánchez-Vega, J.F. Smith, J.L. Taín, R.B.E. Taylor, O. Tengblad, T.F. Thorsteinsen, and the ISOLDE Collaboration, Nucl. Phys. **A654**, 499 (1999).
[25] S. Ćwiok and W. Nazarewicz, Phys. Lett. B **224**, 5 (1989).
[26] S. Ćwiok and W. Nazarewicz, Nucl. Phys. **A529**, 95 (1991).
[27] Y.A. Akovali, Nucl. Data Sheets **58**, 555 (1989).
[28] G.A. Leander and Y.S. Chen, Phys. Rev. C **37**, 2744 (1988).
[29] G. Alaga, K. Alder, A. Bohr and B. Mottelson, Mat. Fys. Medd. Dan. Vid. Selsk. **29**, no. 9 (1955).
[30] V.M. Mikhailov, Izv. Akad. Nauk SSSR, Ser. Fiz. **30**, 1334 (1966).
[31] A.J. Aas, H. Mach, M.J.G. Borge, B. Fogelberg, I.S. Grant, K. Gulda, E. Hagebø, W. Kurcewicz, J. Kvasil, A. Lindroth, T. Martinez, D. Nosek, B. Rubio, J.F. Smith, K. Steffensen, J.L. Taín, O. Tengblad, T.F. Thorsteinsen, and the ISOLDE Collaboration, Nucl. Phys. **A611**, 281 (1996).
[32] B. Ackermann, H. Baltzer, C. Ensel, K. Freitag, V. Grafen, C. Günther, P. Herzog, J. Manns, M. Marten-Tölle, U. Müller, J. Prinz, I. Romanski, R. Tölle, J. de Boer, N. Gollwitzer, and H.J. Maier, Nucl. Phys. **A559**, 61 (1993).
[33] S. Raman, C.W. Nestor, Jr., and P. Tikkanen, At. Data Nucl. Data Tables **78**, 1 (2001).
[34] M. Dahlinger, E. Kankeleit, D. Habs, D. Schwalm, B. Schwartz, R.S. Simon, J.D. Burrows, and P.A. Butler, Nucl. Phys. **A484**, 337 (1988).
[35] J.R. Hughes, R. Tölle, J. de Boer, P.A. Butler, C. Günther, V. Grafen, N. Gollwitzer, V.E. Holliday, G.D. Jones, C. Lauterbach, M. Marten-Tölle, S.M. Mullins, R.J. Poynter, R.S. Simon, N. Singh, R.J. Tanner, R. Wadsworth, D.L. Watson, and C.A. White, Nucl. Phys. **A512**, 275 (1990).
[36] P.A. Butler and W. Nazarewicz, Rev. Mod. Phys. **68**, 349 (1996).
[37] N.J. Hammond, G.D. Jones, P.A. Butler, R.D. Humphreys, P.T. Greenlees, P.M. Jones, R. Julin, S. Juutinen, A. Keenan, H. Kettunen, P. Kuusiniemi,

M. Leino, M. Muikku, P. Nieminen, P. Rahkila, J. Uusitalo, and S.V. Khlebnikov, Phys. Rev. C **65**, 064315 (2002).

[38] J. Kvasil, T.I. Kraciková, M. Finger and B. Choriev, Czech. J. Phys. **B31**, 1376 (1981); **B33**, 626 (1983); **B35**, 1084 (1985); **B36**, 581 (1986).

[39] V.G. Soloviev, *Theory of Complex Nuclei* (Pergamon, Oxford, 1976).

[40] A.I. Levon, J. de Boer, G. Graw, J. Kvasil, M. Loewe, V.D. Valnion, M. Würkner, H. Baltzer, C. Günther, J. Manns, U. Müller, T. Weber, Nucl. Phys. **A598**, 11 (1996).

[41] P. Kálmán and T. Bükki, Phys. Rev. C **63**, 027601 (2001).

[42] T. Mitsugashira, M. Hara, T. Ohtsuki, H. Yuki, K. Takamiya, Y. Kasamtsu, A. Shinohara, H. Kikunaga, and T. Nakanishi, J. Radioanal. Nucl. Chem. **255**, 63 (2003).

[43] P. Möller and J.R. Nix, At. Data Nucl. Data Tables. **39**, 213 (1988).

[44] J. Dudek, Z. Szymański and T. Werner, Phys. Rev. C **23**, 920 (1981).